Acknowledgements

First and foremost, I would like to thank my supervisor at NBI, Lene Oddershede, for her great support and patience both initially on settling on a project and during my work on this thesis. Also, thanks to Michael Sørensen, who helped me start up my work on the biology at the Biocenter and supervised me along the way. I have also benefitted greatly from the fine guidance and many talks with Liselotte Jauffred, who started this project up and with whom I collaborated on the *single molecule studies*. Also thanks to Szabolcs Sempsey for guidance and help in the NBI biolaboratory.

Also, I appreciate all the wonderful students in the optical tweezers group who create the best atmosphere and has been the best company during my work, so thanks to all of you. Thank you to Anders, Ninna and Kamilla for proof-reading my thesis.

Finally, I would like to thank my parents for their neverending support and love.

Table of Contents

Chapter 1

Introduction

Optical tweezers and video microscopy offer the opportunity to study biosystems at the single molecule level. With the help of the techniques fluorescence microscopy and tethered particle motion many properties of the biomolecules DNA, RNA and proteins and their interactions have been investigated resulting in intriguing findings. Many biological processes on the DNA have been probed, among these is transcription by the RNA polymerase, for example, nucleosome–RNA polymerase collisions events[1], RNA polymerase diffusion on DNA[2], transcriptional elongation[3;4], and transcriptional termination[5]. Common for these investigations is the application of a probe, such as a polystyrene bead or a fluorescent crystal, a quantum dot, connected to the biomolecule either to measure the force exerted by the biomolecule, to establish its kinetics or to track it via the fluorescence of a conjugated quantum dot or fluorescent bead.

Fluorescence tracking is also employed in this study, in which we want to monitor the movement of an enzyme, the phage T7 RNA polymerase, on the DNA and to visualise its interaction with other T7 RNA polymerases and eventually other proteins. The overall goal is to investigate transcriptional interference of the T7 RNA polymerase *in vitro* at the single molecule level with optical tweezers and video fluorescence microscopy. The knowledge gained from these investigations will potentially give more insight into gene regulation and into how bio-macromolecules circumvent the crowding of proteins on the DNA molecule.

Untill now most single molecule experiments that employ visualisation of an RNA polymerase, have been performed on the *E coli* RNA polymerase. These are for example the impressive experiments of Wang *et al*[1] and of Finkelstein *et al*[6] recently published. Those single molecule investigations that were performed on the T7 RNA polymerase, measured the enzyme act on DNA by force/extention characteristics[3] or did tracking with fluorescent beads[4]. Thus, so far no active T7 RNAP conjugated to a QD via a streptavidin-biotin bond has been reported and it is therefore the objective of this project to make such a complex in order to track T7 RNA polymerase traffic on DNA and verify its proof of concept in a single molecule experiment.

1.1 Aims

My aims are as follows:

Express and verify the activity of a biotinylated T7 RNA polymerase bound to streptavidin-coated beads and quantum dots.

Monitor the transcription of quantum dot functionalized T7 RNA polymerase on a DNA molecule using video microscopy and optical tweezers.

1.2 Outline

I will begin with an introduction to the experiments. Then follows an introduction namely transcription and transcriptional interference and a short description of the phage T7 RNA polymerase; next the methods employed in the experiments are described, namely: electrophoresis, polymerase chain reaction, tethered particle motion, and the theory of quantum dot fluorescence. This leads to the experiments starting with the ensemble experiments conducted with polystyrene beads and quantum dots; the next chapters introduce the single molecule experiments of tethered particle motion conducted with beads and finally the single molecule experiments of the quantum dot conjugated T7 RNA polymerase.

1.3 Introduction to experiments

1.3.1 Ensemble experiments

In this study of the phage T7 RNA polymerase, the construction of plasmids and subsequent expression of a biotinylated polymerase was all made previously by L Jauffred and S Semsey. The T7 RNA polymerase, however, did not appear active in our laboratory. Therefore the initial step was to repeat the expression of the enzyme and continue the activity tests; this work is summarised in section 5.2–5.2.3. Once the activity of the biotinylated T7 RNA polymerase was verified, the following task was to test the activity of the polymerase when it was bound to streptavidin coated polystyrene beads and quantum dots. The beads were chosen as a first choice due to their easy handling compared to the quantum dots. Since these experiments were not succesful, as chapter 6 will show, an experimental setup with quantum dots was chosen next and the experiments and results are described in chapter 7. These experiments turned out succesful and allowed the introduction of single molecule experiments.

1.3.2 Tethered particle motion and single molecule experiments

A simplified assay using tethered particle motion was employed in order to study the T7 RNA polymerase at the single molecule level. Initially, in order to eventually monitor the RNA polymerase move along a surface tethered DNA molecule, it was essential to gain knowledge on how to look for tethered particles, record and analyse data obtained at the microscope. To ease this learning step, micron sized streptavidin coated polystyrene beads were substituted for quantum dots, since these are easily observed in a microscope. The result of this work is summarised in chapter 8. The next planned TPM experiment introduced quantum dots as the probe by coupling the biotinylated RNA polymerase to streptavidin-coated quantum dots and subsequently make the polymerases stall and accumulate on surface tethered DNA. Possibly, the stalled polymerase/quantum dot complexes could then be viewed in a microscope as an increase in fluorescence as they queue up on the DNA. With some experimental modifications the single molecule investigation turned out succesful and the results are described in chapter 9. Finally follows a conclusion and perspective. Part of the experiments and results presented in the following chapters are summarised in an article recently submitted for publication, see appendix 11.2.

Chapter 2

Transcription and the T7 RNA polymerase

2.1 Transcription

The biological process in which the genetic information encoded in DNA is turned into a protein comprises several reactions and these are decribed in the central dogma formulated by Francis Crick:[7]

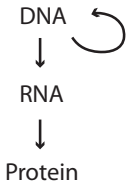

The initial pathway from DNA is divided into two: replication, DNA→DNA, in which a DNA strand is copied by the DNA polymerase into a new DNA strand, which is required, for example, during cell division; and transcription, in which the RNA synthesis is catalysed by the RNA polymerase for the production of messenger RNA. The RNA is in turn translated by the ribosome to finally produce the encoded protein. The bio-macromolecules, DNA polymerase, RNA polymerase, and the ribosome all catalyse polymerisation reactions in which the genetic information is passed on to the product. The present project employs the RNA polymerase and the following section gives a description of the RNA polymerase and transcription.

The RNA polymerase, RNAP, is an enzyme that reads the DNA sequence of a gene from $3'$ towards $5'$ and synthesizes the complementary sequence into RNA from $5'$ to $3'$, a process termed transcription. RNA is a polymer composed of subunits, the nucleotides: ATP, UTP, CTP and GTP, adenosine-, uridine-, cytidine-, and guanosine

triphosphate, also abbrevated A, U, C, and G; A, C and G are also components in DNA together with thymidine, T, whereas U is intrinsic to RNA. The RNA is polymerised in consecutive condensation reactions that each involves binding of a nucleotide, formation of a phosphodiester bond to the nascent RNA, and release of inorganic pyrophosphate. The chemical energy obtained by binding and incorporating a nucleotide is converted into mechanical translocation of the RNAP along DNA.

Transcription can be divided into 3 steps: initiation, elongation and termination, see Figure 2.1.[8] Initiation involves search for the promoter site, which is a specific DNA sequence that the RNAP exhibits enhanced affinity for and at which gene transcription is initiated; it consists of 17 bps that lie upstream of the transcription initiation site.[9] During promoter search the RNAP diffuses along and interacts nonspecifically with the DNA.[2] Upon promoter recognition the RNAP binds to the double stranded DNA and forms a *closed complex* where the DNA remains double stranded. Then the RNAP denatures the double stranded DNA to form an *open promoter complex*, where the melted DNA makes up a *transcription bubble* with the bases exposed for and ready to be copied by the RNAP into complemetary RNA. The DNA opening is a reversible process, where the open and closed complexes exist in equilibrium. After the open promoter complex is formed the RNAP commences *abortive initiation* in which the RNAP synthesises an amount of *oligo* RNAs, which it releases and then return to the promoter site. This process competes with nucleotide incorporation in order to enter *elongation*.

At about 13 nt long newly made RNA the RNAP escapes the promoter and starts elongation forming a *transcription elongation complex*, where it transcribes the full gene. Transcription proceeds in processive steps in which the type of nucleotide is determined by the DNA template and then added to the nascent RNA; by opening a downstream basebair in the DNA helix and the reestablishment of an upstream basepair, the transcription bubble moves along the DNA towards the terminator site. A part of the nascent RNA basepairs with the DNA in the transcription bubble.[10]. Elongation competes with other pathways such as *pausing*, an impermanent conformational state in which the RNAP is unable to elongate, *backtracking* during which the RNAP reverses its translocation on the DNA and stalls, and *termination* in which the RNAP releases the RNA transcript and dissociates form the DNA.[8]

During termination the RNAP dissociates with the DNA template and releases the RNA transcript. The T7 RNAP is destabilised from the DNA by *intrinsic termination*; this means that the termination is signaled by a DNA encoded U-rich RNA transcript, which forms an RNA hairpin that destabilizes the RNAP elongation complex.[5;11] After termination the RNAP is free to enter a new transcription cycle.

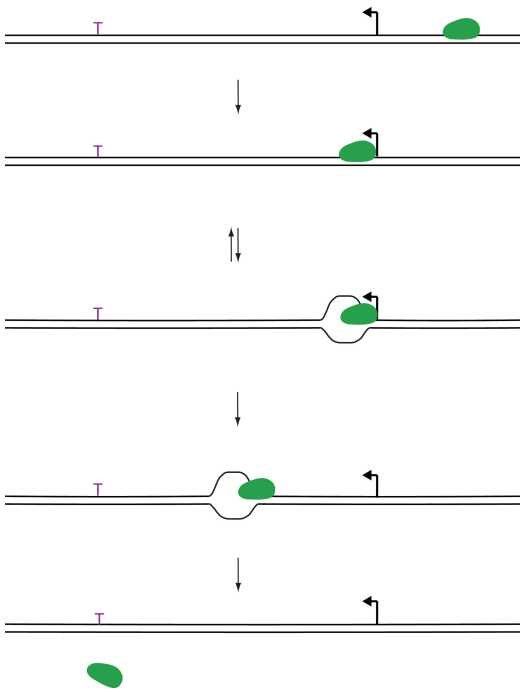

Figure 2.1: *Model of the stages in transcription. From top to bottom: the RNAP diffuses on DNA, recognises the DNA promoter site to which it binds to form a closed complex. The DNA double helix is then opened at the promoter site to form a transcription bubble. After several abortive transcripts where the RNAP synthesise short RNA molecules, the RNAP escapes the promoter site, forms a stable elongation complex and commences transcription of the entire gene. Transcription stops at the terminator site where the RNAP is destabilised from the DNA and the RNA transcript is released.*

2.2 Transcriptional interference

The previous section introduced transcription of the T7 RNAP from a single promoter. However, naturally occurring promoters are often located on different or the same strands of the DNA complicating transcription as one RNAP can interfere with another RNAP either as open complexes or elongation complexes, processes termed *transciptional interference*, TI; thus transcription of one gene can be suppressed by the transcription of another one and in this way TI is involved in gene regulation, see for example the rewiev by Shearwin *et al*[12] (and references herein). The nature of TI depends on the placement of promoters on the double stranded DNA and on the *promoter strength*. Promoters arrangements on the DNA in TI are either tandem (situated next to each on the same DNA strand), divergent but overlapping (facing away from each other on each strand have the promoter sequences overlapping) or convergent (facing each other on each DNA strand). The latter is the focus of this project and a brief introduction follows below on TI caused by converging promoters, however, the concept of promoter strength needs a

short description: the strength of a promoter is determined by how well the RNAP pass from an open complex to an elongation complex (rate of firing).[12] A strong promoter fires more RNAPs into elongation per second than a weak promoter. As stated in the previous section, the open and closed complex exist in equilibrium and the stronger the promoter is the more energetically favorable it also is for the RNAP to form the open complex, thereby promoting transcription rather than the closed complex.[8]

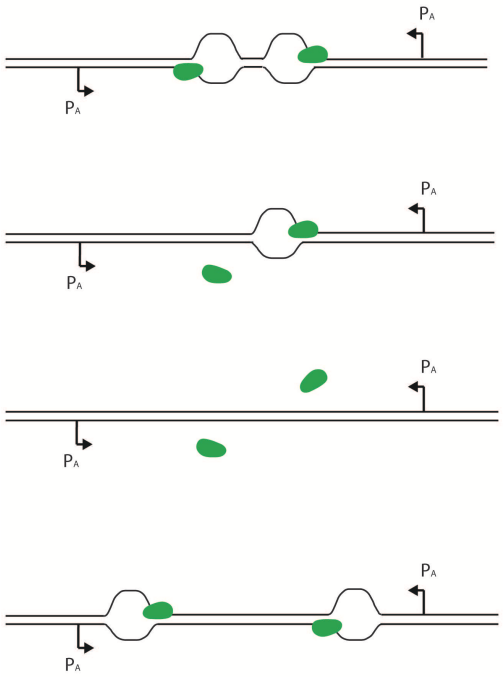

Figure 2.2: *Various scenarios of colliding RNAPs fired from promoters of equal strength. From top to bottom: The two RNAPs collide and stall, one RNAP falls off the DNA and the other cintinues elongation, both RNAPs fall off the DNA, or the RNAPs simply pass each other and continues elongation.*

TI caused by two convergent promoters, one weak and one strong, can result in the following situations:[13] *promoter occlusion*, in which the binding of an RNAP to one promoter that overlaps with another promoter, excludes RNAP binding to the other one; *sitting duck interference*, in which an elongating RNAP from a strong promoter interferes with and destabilises an open complex on the weak promoter, which is slow to shift into elongation, hence termed sitting duck; *collision*, in which two elongating RNAPs collide, which possibly result in ealy termination or stalling of one or both RNAPs. The outlined situations apply to two promoter of different strength, however, when the promoters are equally strong and have the same firing rate, this situation will be different. Several scenarios are possible, see Figure 2.2: the two RNAP stall on the DNA upon collision, one RNAP destabilises and detaches from the DNA and the other continues transcription, both RNAP destabilise and detach from the DNA, the colliding

polymerases somehow pass each other and continue transcription in each direction.

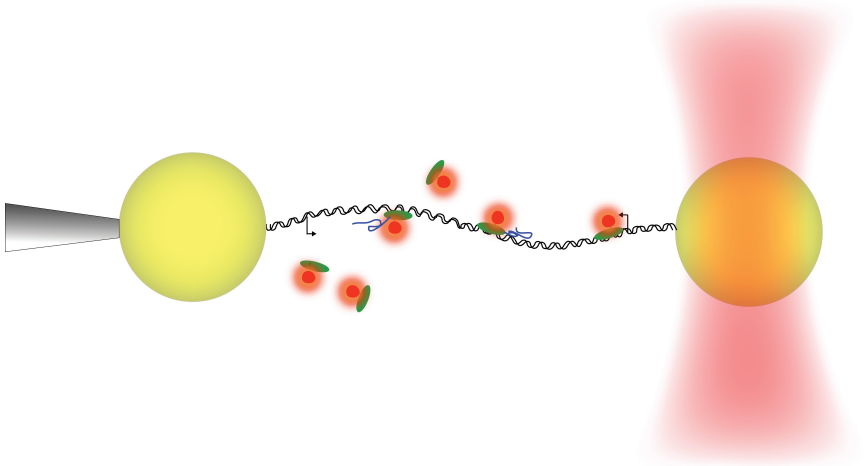

Figure 2.3: *The desired setup of the present project. Two beads, one held by a pipette the other by optical tweezers, are connected with double stranded DNA. The DNA contains two convergent promoters, indicated by arrows, and respective terminators as well. The polymerases (green) bind to the promoters and start elongation to synthesize RNA (blue) and they are visualised with quantum dots (red).*

The intention of this study is to examine collisions of RNAPs fired from two equally strong promoters *in vitro* to gain knowledge on how the RNAPs circumvent collisions with each other. The study relies on quantum dot fluorescence to probe RNAP movement on DNA. The ideal setup for studying collisions of RNAPs fired from convergent promoters is depicted in Figure 2.3. A DNA strand that contains the sequence of two similar but convergent promoters is to be bound at each end to a polystyrene bead. Optical tweezers and a micropipette then trap and fixate each bead and the DNA strand is stretched moderately. RNAPs functionalised with quamtum dots are visualised in a microscope by their fluorescence, which makes it possible to track the RNAPs elongate and collide on the DNA. This setup could potentially yield information on the nature of colliding RNAPs fired from promoters of equal strength.

The desired setup shown in Figure 2.3 requires that the RNAP is active when a quantum dot is attached to it, which has to be tested before the exciting experiments on collision can be conducted; furthermore, the optimal conditions for *in vitro* investigations of the RNAP have to be determined as well. The work presented in the following chapters focuses on these issues. The next section gives a short introduction to the phage T7 RNAP employed in this project.

2.3 The Phage T7 RNA polymerase

The T7 RNAP derives from the bacteriophage T7 that infects *E. coli* bacteria. The *in vivo* elongation rate of a T7 RNAP is ≈200-300 nt/s,[14] which is fast compared to the *E. coli* RNA polymerase that elongates at 50 nt/s.[8] However, the systems are different: the T7 RNAP recognizes the promoter site on its own, unlike multisubunit RNAPs, such as the *E. coli* RNAP, which require the help of a σ-factor to bind to the promoter site. Furthermore, not only does the *E. coli* RNAP require a σ-factor for promoter binding, it is, unlike the T7 RNAP, also regulated by transcription factors that can activate and inhibit transcription.[15] Since T7 transcription is so much faster than that of the *E. coli* RNAP, transcription of the phage genome and expression of the corresponding proteins outruns that of the host and enter the *lytic* stage.

The phage T7 RNAP is a single subunit protein that consists of 883 amino acids, of which the tertiary structure is divided into several domains: the ′palm′, ′fingers′, ′thumb′ and ′N-domain′. The N-domain contains both the N-terminus and residues that recognize and melt the T7 promoter on the DNA. The palm domain arranges two Mg^{2+} ions into the right position for these to catalyse the phophoryl transfer reaction at the active site of the RNAP.[16] As the protein starts elongation and clears the promoter site, it undergoes a conformational change that involves the N-domain where a six-helix-domain rotates 140 °.[17] The x-ray structure of an elongation complex is shown in Figure 2.4, where the polymerase has made a transcription bubble on the DNA; the nascent RNA has disengaged in basepairing with the template DNA and exits a channel.

The T7 RNAP was employed in this project because of the apparent advantage of the fact that it is a single subunit polymerase that does not require any transcription factors. Studies on RNAP collision and the interpretation of data might be complicated if the process involved transcription factors and so the T7 RNAP offer a simple biological setup. Also, as mentioned in the introduction, only few single molecule experiments have been conducted with phage polymerases, which encurage the present study. The genetical construction of the T7 RNAP used in this project is presented in chapter 4.

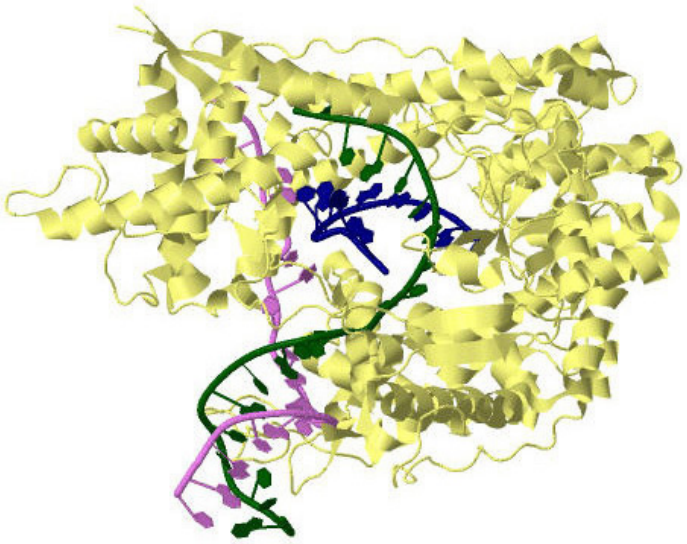

Figure 2.4: *X-ray model of phage T7 RNA polymerase during elongation. Yellow is the T7RNAP polymerase structure, green/purple is the DNA double helix partly unwound by the polymerase to make a transcription bubble. Blue is the nascent RNA. The structure is shown from an angle displaying the RNA exit tract and part of the nascent RNA disengaged in basepairing with the DNA. PDB ID: 1MSW*

Chapter 3

Methods

This chapter introduces the most prominent techniques used in the present biological work: gel electrophoresis and PCR, and in the characterisation of the biological system: TPM and fluorescence video microscopy. The following sections provide a review of each technique and a brief insight into the theory behind them and their applications in this project.

3.1 Electrophoresis

Gel electrophoresis is a method that was greatly used in this project and applied primarily to visualise the RNA product of the T7 RNAP and hence verify enzyme activity. It was also applied for verification of the DNA product from PCR. Furthermore, some interesting properties of QD bound T7 RNAPs were briefly investigated with the technique.

Electrophoresis means *being carried by an electric force* and it is a widely used method to separate molecules according to charge and size. As the name implies, charged molecules can be subjected to an electric field and move along the electric gradient. The velocity, u, of a particle migrating in an electric field in a nonconducting solvent depends on the number of charges, Z, residing on the particle, the strength of the electric field, E and the frictional coefficient, f, of the particle:[18]

$$u = \frac{ZeE}{f} \tag{3.1}$$

where e is the unit charge of an electron. For a spherical particle f is found from Stokes equation:

$$f = 6\pi\eta r \tag{3.2}$$

where η is the viscosity of the medium and r is the radius of the particle. Hence, the mobility of the particle is balanced between the friction of the medium, which counteracts

the particle movement and the electric force of the field on the charge of the particle pulling the particle along.

In gel electrophoresis biomolecules are placed on a gel submerged in a medium containing electrolytes to obtain a current through the system and a buffer to control the pH. When a field is applied to the system the positive molecules will move towards the negative electrode, the cathode, while the negatively charged molecules move towards the positive electrode, the anode. The electrophoretic mobility, $\mu = \frac{u}{E}$ of a particle in a nonconductive medium represents a simple situation, however, electrophoresis is performed in a buffer with ions and at a certain pH. This complicates the equations presented above as the charges residing on the particle will be screened by ions.

A gel consists of a polymer matrix with a network of pores and the molecule migrates through the gel by sieving through the pores. The migration rate of the molecule depends on the pore size: the larger the pore the faster the molecule migrate along the electric field. The pore size is tuned by varying the concentration of the polymer according to each experiment. The retardation of the molecular forward movement in the polymer matrix is a fact not included in the equations above and should be incorporated in the denominator as a function of gel concentration. The most common gel material used in biochemistry is made from the polymers polyacrylamide or agarose. The choice between the two depends on the size of the molecules in question. Polyacrylamide gels have a small pore size with an upper limit of about 80 nm [19] and for very large molecules, agarose gels are preferred yielding a pore size from 50 nm up to well above 300 nm. [20;21]

Electrophoresis is performed with a gel device that casts and holds the gel in place and onto which the electrolyte/buffer solution is added, see Figure 3.1. The device is constructed with electrodes that can be connected to a power supply at constant voltage.

3.1.1 Separation of biomolecules

When gel electrophoresis is applied to biomolecules, the molecular properties have to be considered. DNA has a uniform charge density because each nucleotide in the DNA bears a charge and hence the negative backbone will react to the field and move towards the anode. However, the migration rate of the DNA depends on the length since longer molecules are imposed to greater drag and the molecular conformations are restricted in the gel matrix slowing the DNA down. [18] Many models for the sieving mechanism of DNA through gel pores have been suggested, see for example the review by J-L Viovy. [22] RNA is single stranded and forms secondary structures, which can be circumvented by denaturation to allow size separation on the gel. DNA and RNA are visualised on the gel with Ethidium Bromide, EtBr, which is an aromatic molecule that fluoresces when it is illuminated with UV light. It has a planar geometry that allows it to stack between the bases of the DNA, called intercalation. The driving force of intercalation is due to the hydrophobicity of the aromatic system. [18]

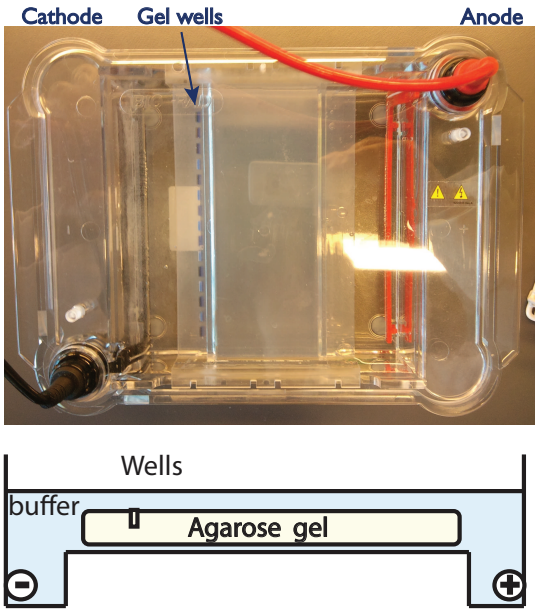

Figure 3.1: *Electrophoresis setup. Top: the equipment consists of a gel casting form placed in the gel electrophoresis holder that contains buffer. The anode and cathode are shown with black and red respectively. Bottom: drawing of the gel with wells formed by a comb.*

Running proteins samples through a gel is not as simple as with DNA. Proteins have different shapes and charge and in order to circumvent this, the proteins are denatured into a polypeptide chain with sodium dodecyl sulfate, SDS, that is anionic and disrupts noncovalent bonds and binds to the peptide. The excess negative charges of SDS make

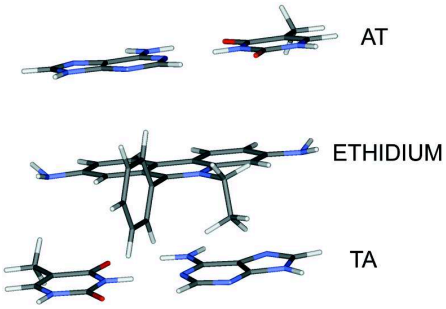

Figure 3.2: *Model of Ethidium Bromide/DNA stacking that shows the T-A and A-T bases on the DNA intercalated with the fluorophore. Image from Reha et al.*[23]

the polypeptide chain uniformly charged and it therefore migrates towards the anode according to size only. Running gels with proteins under native conditions will separate them not only according to size but also according to charge. Proteins exist as zwitterions as they contain both the acidic carboxylic group and the basic amino, guanidino and imidazole groups in their amino acid sequence and so they have electric properties that are intrinsic to each of them according to their sequence composition. At low pH the acid group is neutral whereas the basic groups are protonised, see Figure 3.1.1; reversely at high pH the acidic group is deprotonised whereas the basic group in neutral. At a certain

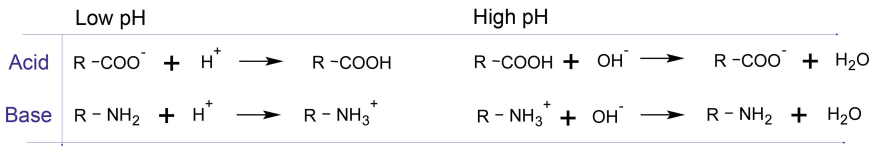

Figure 3.3: *Reaction scheme of acidic and basic groups in the polypeptide chain shown at low and high pH respectively. The amino acids aspartate and glutamate contain the acidic carboxyl group and lysine, arginine and histidine contain the basic amino, guanidino and imidazole groups respectively.*

pH the protein has equal positive and negative charges, leaving the protein electrically neutral (isoelectric). Hence proteins separated in an electric field can also be dispersed according to their isoelectric point if they are allowed to move in a pH gradient. In a buffer with constant pH, the pH must be adjusted according to the isoelectric point of the protein in order to protonize/deprotonise it, otherwise the protein carries no net charge and does not move in the electric field.

3.2 Polymerase chain reaction

Polymerase chain reaction, PCR, is a technique used for amplification of DNA and it was therefore vastly applied in the present work for producing the DNA designed for both the ensemble and single molecule experiments. The experiments rely on DNA of a defined length with or without promoter and terminator sites and sometimes functionalized at the 5' or 3' ends using special primers.

In order to amplify a DNA sequence the reaction is performed in a buffer containing Mg^{2+}, nucleotides, DNA polymerase, and the DNA template. The PCR cycle[24] is as follows: two oligonucleotides, the primers, are designed with complementary basepair sequence to the primer binding sites at the $3'$ ends on each side of the gene on the double stranded DNA, see Figure 3.4. When the DNA is heated beyond its melting point up to 95 °C, the two strands separate, which allows the primers to bind to their complementary sequence on each strand. Lowering the temperature to just below the melting point of the primers makes them anneal to their complemetary sequences. The *taq* DNA polymerase is a heat resistant enzyme that tolerates repeated heating without denaturising. A raise in temperature to about 70 °C makes the DNA polymerase extent the primers in each direction towards the 5' end, which results in two separate pieces of DNA containing the target gene. The two new pieces of DNA are then heated again to denature the strands and now 4 primer binding sites are available for the primers to bind. The cycle is repeated 20-30 times and the amount of DNA pieces grows exponentially untill the reaction is stopped by lowering the temperature to 4 °C.

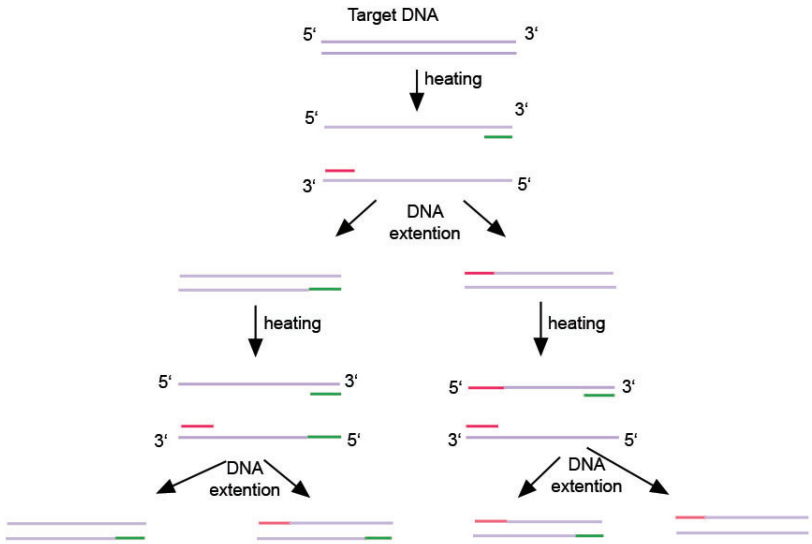

Figure 3.4: *The polymerase chain reaction. The target DNA is denaturised by heating and the primers bind (red and green). The primers are extented by the DNA polymerase and two new pieces of DNA are made. These are then reheated for primers to bind the complemenary site and next extended to make four new pieces of DNA. The cycle is repeated till the DNA is amplified sufficiently.*

PCR is performed by a thermal cycler, a heating apparatus designed to regulate the temperature in time intervals needed for the specific target gene. The optimal temperature, denaturation- and synthesis time depend on the target gene to be amplified and are best determined empirically.

3.3 DNA purification

After running PCR, the amplified DNA needs to be purified and the chosen purification procedure depends on requirements of the subsequent experiment. In the present project the DNA was purified by two different commercial purification kits: a spin column kit (Fermentas) and a gel extraction kit (Qiagen). The first is based on spin column with a build-in silica membrane that DNA binds to; the PCR product is transferred to the spin column to let the DNA interact with the membrane and the presence of the chaotrope, guanidinium thiocyanate, inactivates any proteases in the solution.[25] Afterwards, the column is flushed with a wash buffer that contains ethanol; the wash removes the denaturised proteins as well as the nucleotides, and salts and the DNA is subsequently eluted from the silica with a buffer and collected. The binding buffer containing the chaotrope, wash buffer, and elution buffer are all supplied with the kit. The second purification

procedure was gel extraction: this was used to obtain higher purity as the entire PCR reaction is subjected to gel electrophoresis in order to separate the desired fraction of DNA product from other DNA derived from preterminated polymerisation, primers, proteins and dNTPs. The gel band corresponding to the desired DNA is cut from the gel and dissolved with a special buffer provided with the purification kit. The mixture is loaded onto the a spin column as described above and the DNA eluted similarly.

3.4 Tethered particle motion

Our project applies tethered particle motion, TPM, to monitor biotinylated T7 RNAPs bind and transcribe DNA in a microscope. As the technique relies on the properties of the tether, in this case DNA, it is also reasonable to briefly touch upon theoretical modelling of the polymer and its characteristics, in order to estimate some values for comparison of the experimental results presented in chapter 8.

The single molecule technique, TPM, is a method that uses a DNA molecule tethered at one end to a surface and the other end to a particle e.g. a polystyrene bead, fluorescent bead, gold particle, or a quantum dot, see Figure 3.5. The particle motion is then observed and recorded by video microscopy. The observed restricted random walk of the surface tethered particle reflects the conformations of the DNA. As depicted in Figure 3.5, the spring force of the DNA tether, F=-κx, acts on the bead and pulls it towards the point of surface attachment; the bead is also subjected to thermal energy resulting in Brownian motion and a viscous drag of the surrounding medium. Experimentally the positions of the DNA tethered particle are obtained by extracting the x and y coordinates of the particle centre from a recorded image sequence; hence the (x,y) values correspond to the three dimensional positions of the particle projected down onto the image plane at different time points. The x and y positions can be plotted in a histogram to show the distribution.

TPM is applied in the study of biological macromolecules such as proteins and enzymes acting on DNA, for example in transcription regulation. In these studies, proteins or enzymes acting on the DNA cause a change in the DNA excursions and hence a shift in the x and y-distributions. For example, this change could be caused by DNA looping by the Lac repressor;[26] looping by the Type IIE restriction enzymes NaeI and NarI;[27] DNA bending by TATA binding protein,[28] or by surface immobilised *E coli* RNA polymerases binding and transcribing bead tethered DNA, thereby fixing the DNA at the surface and decreasing the tether length upon transcription.[29] Common for these experiments is that the change of the particle motion upon enzyme interaction with the DNA is observed in real time. Kinetic parameters can be extracted from the data such as association and dissociation constants, loop formation rates, and transcription rates.

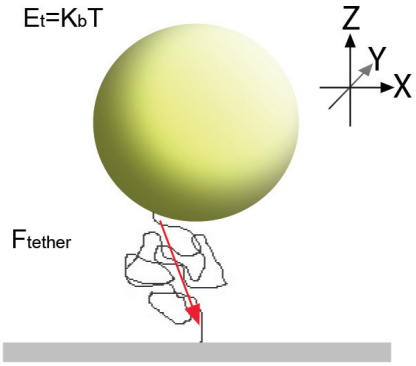

Figure 3.5: *Bead tethered to a surface with DNA. The surface lies in the the xy-plane. Shown are the thermal energy, $E_t = K_bT$ responsible for thermal fluctuations of the bead and the tether force that pulls the beads towards the surface.*

3.4.1 DNA and polymer theory

A DNA molecule in a buffer solution is randomly coiled and can take a number of conformations with similar energy.[30] The polymer can be approximated to an ideal chain in *3* dimensions, which is described with N segments of equal Kuhn lengths of L_k=2ξ, where ξ is the persistence length, that are allowed to overlap and have random orientation; then NL_k correspond to the contour length of the polymer. The mean square end-to-end displacement, $\langle \mathbf{r}^2_{ee,xyz} \rangle = NL_k^2$ of an ideal chain free in *3* dimensions determines the mean volume that a randomly coiled DNA molecule occupies.

The DNA is elastic and energy is required to stretch it away from r_{ee} and therefore such conformations are less probable. When DNA is stretched below its contour length, L_c, the polymer acts like a spring and Hookes law applies: F=-κx, where F is the spring force, κ is the spring constant and x is the displacement from the equilibrium. To examine the properties of DNA in *3* dimensions, the model is broken down into 3 1D conformations in x, y, and z by projection onto the respective axes. In this case the probability distribution of configurations in 1D is:[30]

$$P(x) = \frac{1}{\sqrt{2\pi\sigma^2}} e^{\frac{-r^2_{ee_x}}{2\sigma^2}} \quad , \tag{3.3}$$

where the variance $\sigma^2 = N\langle L_k^2 \rangle$ and $\langle L_k^2 \rangle$ is the expectation of projection of segments onto the x-axis. The probability distribution of an ideal chain is Gaussian and usually data obtained from TPM experiments is fitted with such a distribution. However, the fit is an approximation only, since no heed is payed to neither excluded volume effects, where two parts of the same DNA cannot occupy the same space, nor to the attached bead and surface, which complicates the fitting.

3.4.2 DNA excursion

Projection of all the segments of the polymer onto the (x,y)-plane corresponds to the situation of a TPM experiment, and the most likely value of $\langle \mathbf{r}^2_{ee,xy} \rangle$, r_{ee}, is found by:[30]

$$r_{ee} = \sqrt{2/3}\sqrt{NL_k} \quad , \tag{3.4}$$

As with P(x), this expression does not take excluded volume effects into consideration, in which a larger r_{ee} is expected. Furthermore, the DNA is neither attached to a surface nor a bead, which changes the available conformations; in addition, the size and geometry of the bead also influence the experimental values.

In practice one way of estimating the mean value of excursions from experimental TPM data, is by employing the root mean square deviation:

$$RMSD = \sqrt{std_x^2 + std_y^2} \quad , \tag{3.5}$$

where std_x and std_y are the standard deviation in x and y respectively:

$$std_x = \left(\frac{1}{n-1} \sum_{i=1}^{n} (x_i - \bar{x})^2 \right)^{\frac{1}{2}} \quad , \quad std_y = \left(\frac{1}{n-1} \sum_{i=1}^{n} (y_i - \bar{y})^2 \right)^{\frac{1}{2}} \quad , \tag{3.6}$$

where $\bar{x}$ and $\bar{y}$ are the mean of x and y. RMSD relates the magnitude of deviation to the mean of positions and thus gives the mean excursion by the bead from the point of surface attachment corresponding to the theoretical, r_{ee} presented above. RMSD is employed in the statistical analysis of TPM data in chapter 8.

3.5 Quantum dots

Quantum dots are applied in tracking of proteins *in vitro*[6;31] and in *in vitro and in vivo* immunofluoresence[32;33] studies. In the present project quantum dot fluorescence was used as a means of tracking enzymes, hence an introduction to the fluoresence properties of QDs will be touched upon here, providing a brief explanation of the size dependence of QD fluorescence.

Quantum dots are crystals made from semiconductor material in the size range of a few nm to hundred nm.[34] They consist of only a few thousand atoms and typically have a spherical or rod like geometry. Semiconductor material is characterised by having a valence band and conductance band separated by an energy bandgap, as opposed to conductors, such as gold, in which the two bands coincide, see Figure 3.6 a) and b). Therefore, it requires energy to excite electrons from the valence to the conductance band. When the electron is excited to the conductance band it leaves a hole behind in the valence band with positive charge and the pair is called an *exiton*; the electron and hole are mobile in their respective bands in bulk semiconductor material. Due to the

small size of the quantum dot, the energy levels in the valence and conduction bands do not form a continuum but are separated, Figure 3.6 c). The electron (and consequently the hole) is excited to a descrete energy level and decays back to the lowest unoccupied level in the valence band with the resulting narrow spectrum of emitted radiation. The quantized energies can be found for an electron in a sphere by solving the Schrödinger equation:[35]

$$E_n = \frac{n^2 h^2}{8 m_e R^2} \quad , \tag{3.7}$$

where n is the quantum number, m_e, the electron mass, and h the Planck constant.

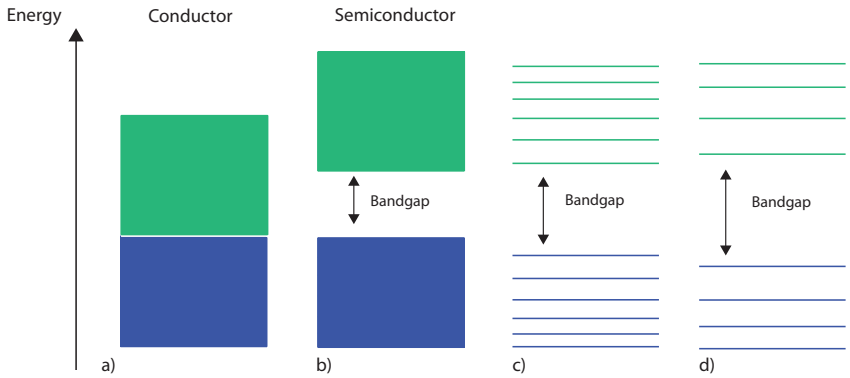

Figure 3.6: *The valence and conductance band of a bulk semiconductor, b), are separated by a bandgap unlike those of conductor, a), that coincide. The electron states in a quantum dot are separated with discrete energies as depicted in c) and d). c) corresponds to the energy levels of a QD that is larger that the one represented by d).*

The colour of the QD emission light is tunable as it strongly depends on the size of the crystal, which determines the confinement of the exiton. The energy of the exiton in a sphere is given by:[35]

$$E_{ex} = \frac{h^2}{8R^2}\left(\frac{1}{m_e} + \frac{1}{m_h}\right) - \frac{1.8e^2}{4\pi\varepsilon R} \quad , \tag{3.8}$$

where m_e and $m_h$the electron and hole mass respectively, R is the QD radius, e is the unit charge of the electron, and ε is the permittivity of the medium and R is the radius of the sphere. The first term defines the kinetic energy of the exiton and the second term the Coulomb interaction of the elctron and hole. The size dependence of the emmitted radiation from a quantum dot is seen from equation 3.8. The energy depends on the reciprocal of the second power of the radius, which means that the smaller the QD is, the farther the energy levels lie from each other and the larger the bandgap gets with the

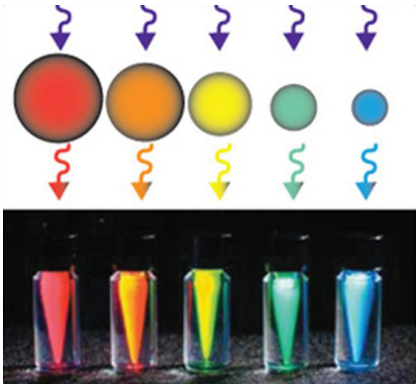

Figure 3.7: *Fluorescence of quantum dots of various size ranging from red to blue emission with higher energy. Image from Invitrogen.*

consequence that the emission light shifts towards a shorter wavelength, see Figure 3.6 d).Figure 3.7 shows the fluorescence colour of various sizes of wuantum dots in solution.

Chapter 4

Genetics of a tagged T7 RNA polymerase

The T7 RNAP employed in this project is modifed at the N-teminal with a two tags, thus potetially altering the enzyme kinetics; however, previously the T7 RNAP was modified with one tag and it was shown that it retained activity.[36] The genetic construction of the T7 RNAP and the biological system for its expression were designed by S Sempsey with the aim of functionalising the enzyme with a particle. The His_6-tag and the Bio-tag presented below are common genetic tags in biotechnology, commercially available and used for purification, functionalisation and quantification of proteins.

The plasmid, pBH161, was previously obtained from William T. McAllister and encodes a T7 RNAP His_6-tagged N-terminally.[36]. The enzyme was further tagged at the N-terminal by S Sempsey and L Jauffred with a 15 amino acid (aa) sequence, GLDIFEAQKIEWH, referred to here as Bio. This peptide had been selected by screening a peptide library for sequences that the enzyme, biotin ligase, modifies with a biotin molecule.[37] Biotin ligase forms an amide bond between the carboxyl group on biotin and the ε-amine on a single lysine in the carboxyl carrier protein, a subunit of acetyl-CoA carboxylase.[38] The selected peptide, Bio, also contains a single lysine that is recognised and biotinylated *invivo* by biotin ligase.

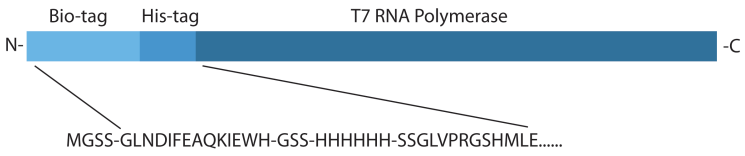

Figure 4.1: *Construct of the biotinylated T7 RNAP showing the N-terminal aa sequence. The N-terminal part of the enzyme begins with the 15 aa sequence recognised by biotin ligase. Then follows a 3 aa spacer and the His_6-tag whereupon the aa sequence of the T7 RNAP begins.*

Between the Bio-tag and the His_6-tag is a 3aa spacer of SGG and the His_6-tag is separated from the T7 RNAP sequence with a 13aa spacer, see Figure 4.1.

The bacterial strain BL21Star(DE3) (Invitrogen), genotype: F^- *ompT* $hsdS_B(r_B^- m_B^-)$ *gal dcm rne131*, was used for expression of the modified enzyme and contains the gene of a *wt* T7 RNAP under lac respressor control, see Figure 4.2. The strain had been transformed with two plasmids: the pBioT7 with the modified Bio T7 RNAP under lac-repressor control and pBirA (Avidity) containing the gene for biotin ligase downstream a T7 promoter. The plasmids infer immunity to the antibiotics chloramphenicol and ampicillin. When isopropyl β-D-thiogalactoside, IPTG, a lactose analogue, is mixed with the cell medium it inhibits LacI and the expression of *wt* T7 RNAP and Bio T7 RNAP is induced; the former transcribes the gene for Bio T7 RNAP and biotin ligase and biotinylation of Bio T7 RNAP commences.

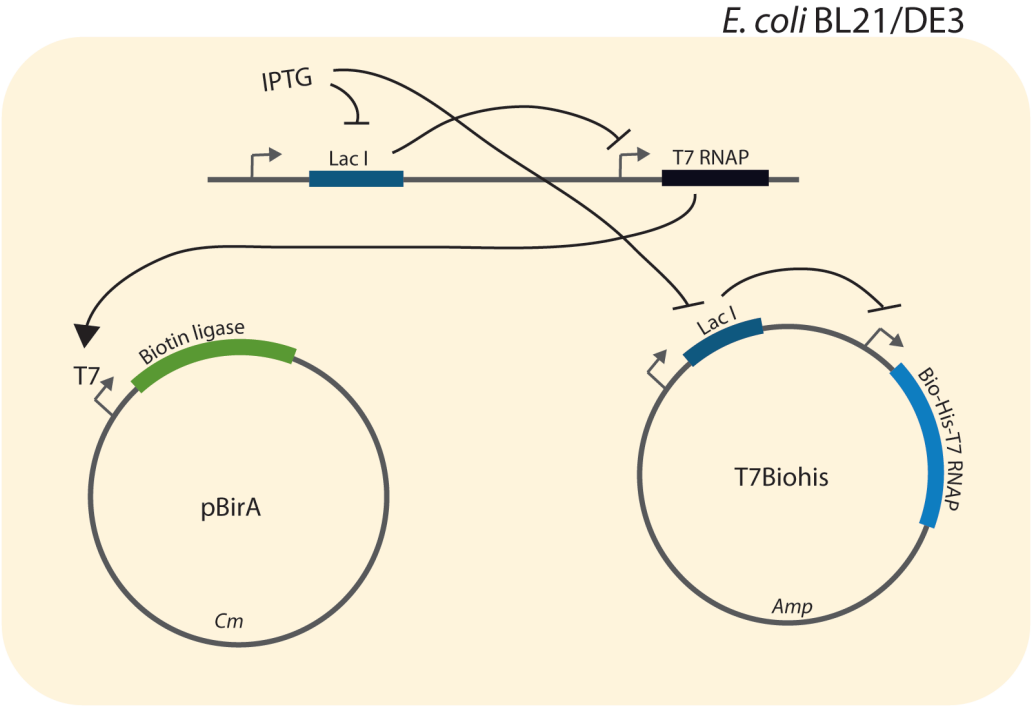

Figure 4.2: *The BL21/DE3 strain transformed with the plasmids, pBirA encoding biotin ligase and T7Biohis carrying the gene for the bio-tagged T7 RNAP. Wild type and Bio T7 RNAP are both under LacI control. In the presence of IPTG LacI is repressed and the two types of polymerases are expressed as well as biotin ligase.*

The next chapter presents the results of the expression and purification of the T7 RNAP.

Chapter 5

Ensemble studies of a biotinylated T7 RNA polymerase

This chapter introduces the preliminary work on the T7 RNAP including the biotinylation method, activity test and buffer adjustment. Previous attempts to verify the activity of both a specifically and nonspecifically biotinylated T7 RNAP had failed in our laboratory, so a reasonable start on the project was to embrace this problem by examining the conditions for polymerase transcription and the choice of biotinylation. All experiments were made at the Biocenter in the laboratory of M A Sørensen. Section 5.2 through 5.2.3 are part of a 'fagproject', see appendix LADIDA, and a summary is included here as an important background for the work presented in the following chapters.

5.1 Biotinylation

A first approach was to question the chosen biotinylation method. Previously, nonspecific biotinylation of a commercial T7 RNAP chemically with *BiotinTag, Micro-Biotinylation Kit* (Sigma) failed, so in order to seek a solution to this, the experiment was repeated. The BiotinTag Kit utilises biotinamido hexanoic acid 3-sulfo-N-hydroxysuccinide ester, BAC-sulfo-NHS, which reacts with free amino groups on a protein to form an amide bond. In this respect it was neccesary to consider the amount of amino acids with primary amines in the polymerase, namely lysines. The T7 RNA polymerase contains 60 lysines: 3 in the specificity loop, aa 739-769, responsible for sequence specific contacts with base pairs in the promoter region, 8 lysines in the promoter binding region, aa72-150 and aa 191-267, that interact with the 17 bp promoter and the rest in the palm and finger domain.[39] In order to avoid biotinylation of the T7 RNAP in the binding tract, BAC-sulfo-NHS might be excluded from this region by adding junk DNA (hering sperm) to the reactants. The intention was that the T7 RNAP would nonspecifically interact with

the DNA thus making it less likely that the DNA binding region of the enzyme would react with BAC-sulfo-NHS. The experiment failed for other reasons possibly because the T7 RNAP disappeared after being dialysed as the working concentration was too small.

Nevertheless, the above considerations readily pointed out the necessity for an alternative biotinylation method, mainly because the outcome otherwise most likely would be a T7 RNAP population with nonhomogenious activity. As the focus of this project is to examine polymerases acting on DNA containing two opposed but equally strong promoters, nonspecific biotinylation would compromise this approach, because biotinylation of different points on the protein might alter binding and transcription rate of the polymerase and hence promoter strength, which is crucial to this project; therefore, to avoid any possible complications in this respect, specifically biotinylation was preferred and the above method was abandoned.

A specifically biotinylated T7 RNAP was previously constructed, purified and tested for activity by S Sempsey in Hungary. An amount of this was sent to our lab, however, storage conditions, purity and concentrations were not established. To control the conditions better, expression and purification of the biotinylated T7 RNAP in our own laboratory was preferred and this was decided upon. The following sections describe the procedure and results.

5.2 Experimental

5.2.1 Expression & Purification of T7 RNA polymerase

A commercially developed Ni^{2+}-agarose resin (Qiagen) was used to separate the Bio-T7RNAP from other expressed proteins in the cell. The construction of the polymerase with a His_6-tag takes advantage of the specific binding of the tag to Ni^{2+}, which allows easy purification. The His_6-tagged T7 RNAPs will stay in the Ni^{2+}-resin, which can be washed in order to remove any additional proteins, DNA etc. coming from the cell lysate. The enzyme is then eluted using molar excess of imidazole, a molecule also constituted in the histidine side chain, which competes with the His_6-tag for the Ni^{2+} binding sites.

Enzymes were purified from the cell lysate with the procedure described in appendix 1. In order to estimate the enzyme concentration the ExPASy ProtParam tool[40] was used to find the theoretical extinction coefficient of the Bio-T7 RNAP. The extinction derives from the amino acids containing aromatic compounds: tyrosine, tryptofane and phenylalanine, which cause a 280 nm absorbance due to π–π^* electronic transitions in the aromatic ring. The absorbance of the enzyme solution was measured using a Nanodrop spectrophotometer (ThermoScientific) and the approximate enzyme concentration was subsequently estimated to be 26 μM employing the Beer-Lamberts equation.

The fraction of biotinylated enzymes was previously determined by S Sempsey to be 95-99% of the total amount of expressed enzymes. The estimate relied on an affinity purification using an avidin resin, SoftLink Soft Release (Promega), which was placed in a chromatography column and centrifuged in order to collect the flowthrough that might contain non-biotinylated T7 RNAPs. An SDS gel revealed that only very little, $\approx$ 1-5% of the enzyme showed up in the flowthrough and none in the proceeding washings.

5.2.2 Activity

Due to possible contamination of RNase, which is an enzyme that degrades RNA,[41] RNase inhibitor was added to the transcription buffer, a protein that binds tightly RNases noncovalently.[42] Once established, the following reaction mixture was used as a standard throughout the project. It contained 2 ng/μl 1000 bp DNA template with T7 promoter and terminator, 1×transcription buffer (40 mM Tris-HCl (pH 7.9), 6 mM $MgCl_2$, 10 mM NaCl), 2 mM spermidine, 10 mM DTT, 2 mM of each rNTP, 2 u/μl RNAsin, 2.6 μM Bio-T7RNAP. The activity test was made at 37 °C for 1 hour, stopped with load buffer (4% Ficoll400, 0.33 mM EDTA, bromophenol blue) and the product ran on 1.8 % agarose gel in 1×PB at 120V for 50 min.

5.2.3 Results

Figure 5.1 shows the result of the enzyme purification. Column 1 is the lysate of cells that contain the plasmids pBirA+T7Biohis and express the T7 RNAP, column 2 is that of the control with cells containing pBirA only. Column 3-8 show the Ni^{2+}-agarose resin wash of 1 (T7) and 2 (control) with respectively 2,4 and 6 bed volumes of buffer and they show increasing purity. Eluation of T7 RNAP, red arrows, and the corresponding control with respectively 50 mM (column 9-10), 80 mM (column 11-12), 100 mM (column 13-14) and 200 mM imidazol (column 15-16) reveal that the enzyme elution peaks at 80 mM imidazol and this is then chosen as the working stock. Green arrows indicate an unspecified polypeptide with similar affinity for the His_6-tag.

Figure 5.2 shows the activity of the 80 mM imidazole eluate in a dilution series from 2.6μM, lane 1, to 26nM, lane 6. T7 RNAP activity is visible even at a 1000 fold dilution of the stock, lane 6. As expected the RNA product decreases with increased dilution. Note that the template at high T7 RNAP concentration, lane 1-3 especially, is dragged downwards in the gel suggesting that the T7 RNAP is still associated with the template, thereby possibly increasing migration due to extra charges residing on the enzyme at the given buffer pH. This fact is discussed further in chapter 7.

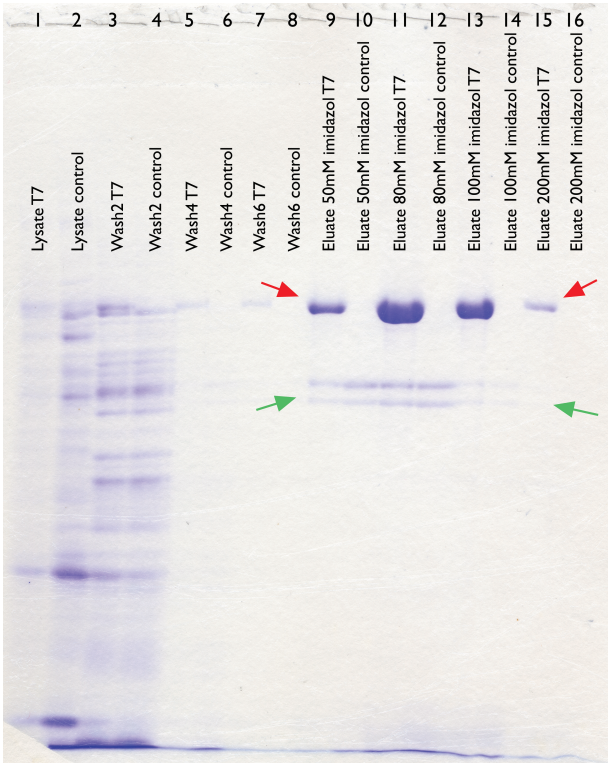

Figure 5.1: *Purification of His_6-tagged and biotinylated T7 RNAPs. Lysate from cells containing both plasmids is denoted 'T7', column 1; for control cells lacking the plasmid with the biotinylated T7 RNAP are used, column 2. Column 3-8 are the resins washed 2, 4, and 6 times the resin volume. Some T7 RNAP is eluted at 50 mM imidazol, however the major part is eluted at 80 mM and some at 100 mM and almost none is left at 200 mM.*

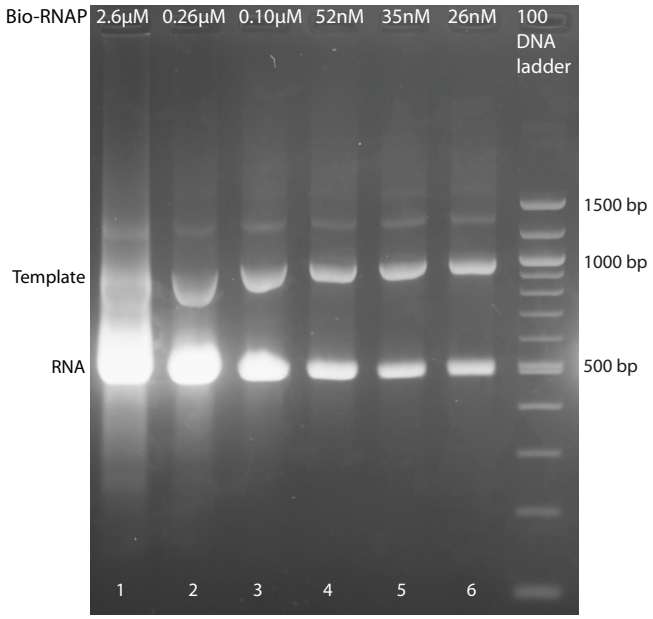

Figure 5.2: *Activity of 80 mM imidazole purified T7 RNAP. The 26μM T7 RNAP stock was diluted to the concentrations: 2.6μM, 0.26μM, 0.104μM, 52nM, 35nM and 26nM, the activity of which are shown in lane 1-6 respectively.*

5.2.4 Optimisation of transcription buffer

Since many single molecule experiments use different salts and salt concentrations, simplified transcription buffers and procedures at room temperature instead of 37 °C, this incited an investigation of the influence of temperature and various chemical components on transcription.

The activity procedure given above was used as a standard for these tests, while some of the buffer contents were varied. Firstly, since the single molecule studies as a first approach was to be performed at room temperature and at a concentration of each rNTP of 0.5 mM, these conditions were tested in combination. Secondly, the effect of 10 mM NaCl, 2 mM spermidine, α–caseine, BSA and QDs was tested: NaCl and spermidine in order to see if these were indispensible; α–caseine and BSA because these were to be used as blocking agents in the chamber setup of the single molecule studies and when working with beads and QDs in order to minimise nonspecific surface interactions; also an additional beneficial effect of BSA and α-casein is their screening of the enzyme from protease degradation. QDs were tested because their presence could influence enzyme activity even when these are not bound to the T7 RNAP.

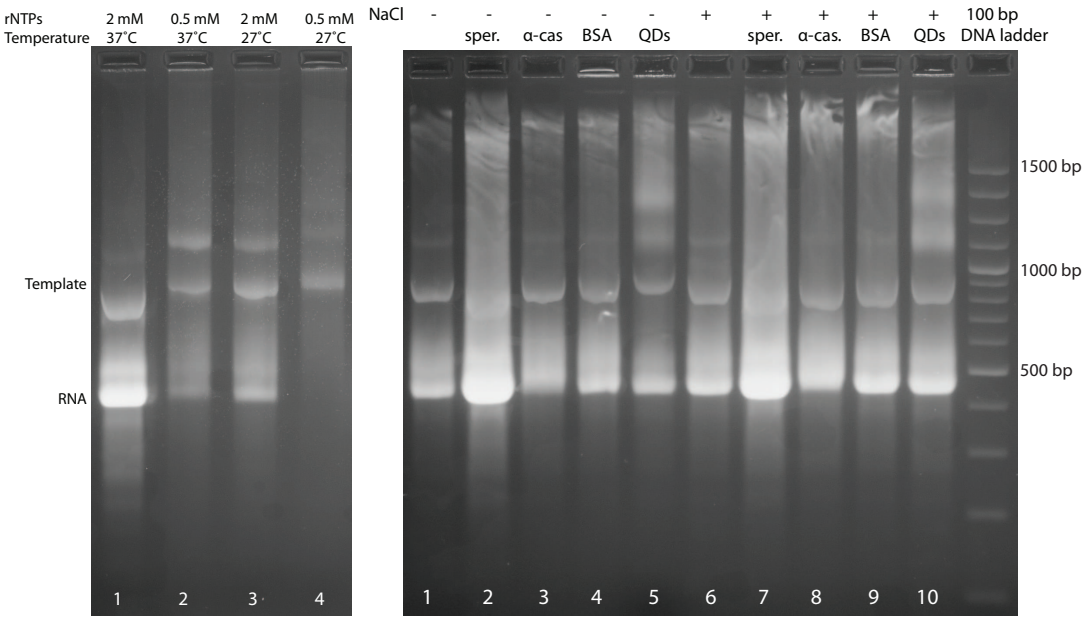

Figure 5.3: ***(a)*** *The effect of temperature and nucleotide concentration on activity. Lane 2 and 4 show that lowering rNTP concentration has the greatest effect.* ***(b)*** *Activity test with varying buffer components: Lane 1–5 and 6–10 are respectively without and with NaCl. Lane 1 and 6 are activity test in bufer only. Generally spermidine and BSA enhanced activity, whereas the amount of RNA product in the samples containing α–caseine, lane 3 and 8, decreased compared to lane 1 and 6.*

5.2.5 Results

Lanes 1 and 2 in Figure 5.3**a** show activity at 37 °C with 2 mM and 0.5 mM nucleotides, respectively. Lanes 3 and 4 show the same samples tested at 27 °C. It is clear that a combination of decreased nucleotide concentration and temperature results in a substantial decrease in activity. Particularly, the decrease in rNTP concentration to 0.5 mM limits the RNA product more than lowering the temperature, most likely a consequence of the rNTPs being reactants in the polymerase chain reaction and hence a limiting factor, whereas decreasing temperature only slows the reaction. Figure 5.3**b** shows that the presence of the salt, NaCl, increases activity to some extent, maybe due to some stabilising effect on T7 RNAP–DNA interactions. The most dramatic increase happens in the presence of spermidine. Spermidine is cationic at physical pH and interacts with the negative phosphate backbone of DNA at the DNA groove stabilising the DNA helix.[43;44] It is also clear from the test that BSA is preferable over α-casein, compare lanes 3 and 4, 8 and 9. Adding QDs to the polymerases has only a minor effect on the activity as seen in lanes 5 and 10. On the basis of the results, NaCl, spermidine and BSA were included in the reaction buffer used in the succeeding experiments.

Chapter 6

Ensemble studies of a bead bound T7 RNA polymerase

In chapter 5 the present work verified that the specifically biotinylated T7 RNAP was indeed active and more importantly established the conditions for attaining optimal purity and enzyme concentration. Next the challenge was to verify that the specifically biotinylated T7 RNAP was also active when functionalised with a particle via the bond between the biotin molecule on the T7 RNAP and streptavidin on the particle surface. As with the TPM experiments presented later in chapter 8, which employed polystyrene beads as a first approach to working with the single molecule technique, beads were likewise applied here because they are easier to handle than QDs: firstly, their size in the micrometer range makes them easy to centrifuge down in a suspension when they are to be separated from the supernatant, as they are visible to the eye and appear as a white pellet when centrifuged. Secondly, they do not require UV equipment for detection as the QDs do. In the light of these advantages it was furthermore presumed that the polystyrene beads and QDs could be used interchangeably, since the biotinylated RNAP would bind to the streptavidin molecule irrespective of the surface it was attached to.

6.1 Considerations

An outline of the experiment is given in Figure 6.1. After the RNAPs bind to the streptavidin binding sites, the beads are to be washed and then subjected to the activity procedure presented in section 5.2.2. The control is to undergo the same procedure as the samples but is to be incubated with biotin in order to block all binding sites on streptavidin thereby excluding the T7 RNAP from binding.

In these experiments beads of 0.51 μm diameter were used (Bangs Lab) having a surface area of 0.817 μm^2. The beads were conjugated to tetrameric streptavidin molecules

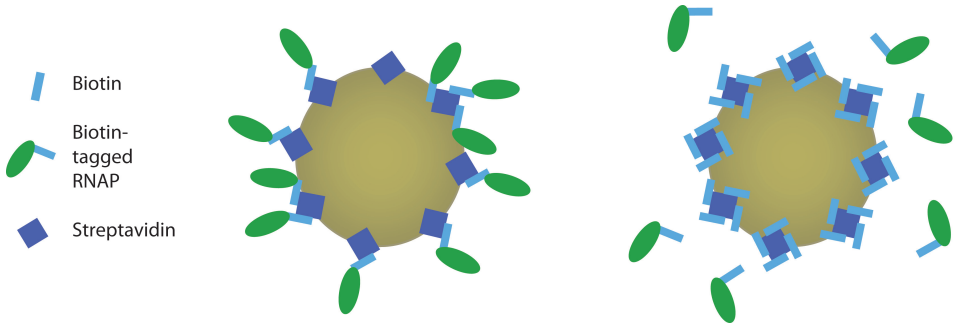

Figure 6.1: *Schematics of biotin saturation of streptavidin coated beads. Left: T7 RNAP binding to streptavidin. Right: Biotin molecules compete with the T7 RNAP for streptavidin binding sites and block RNAP-streptavidin bond formation.*

and came in MES buffer containing 0.1 % BSA. Given the data supplied by Bangs Lab the biotin binding capacity in 1 μl bead suspension was determined to be 2.116 *10^{15} molecules corresponding to 3.514 mM.

Generally in order to avoid nonspecific binding of the biomolecules to the bead surface and sticking of beads to the eppendorf tube, the beads were incubated with BSA before binding RNAP. Furthermore, it was determined from preliminary experiments that 10 μl was the minimum amount of beads possible to work with. For example, the beads were generally lost during the process when working with 5 μl only, as they stuck to the tube surface in spite of the addition of BSA to avoid this. Also the volume of washing buffer and the number of washings were restricted as it made the beads difficult to centrifuge down because they tended to stick to the tube surface; hence the larger the surface was the more beads were lost in the subsequent steps of the procedure.

The concentration of Bio-RNAP, 26 μM stock, is substantially lower than the hypothetical amount of biotin binding sites on streptavidin in 10 μl bead suspension. To this end, the volume of T7 RNAP added to the beads was also constrained as the RNAP solution contained 50 % glycerol, which made the beads hard to centrifuge down. Therefore the RNAP solution had to be diluted below 10 % glycerol. The RNAP concentration was quite low compared to that of streptavidin and previous tests had shown that altering the concentration in this regime, for example from 0.86 μM to 4.3 μM had no effect on the RNA product in the subseeding activity tests.

A reasonable degree of blocking was expected with an equimolar concentration of biotin to biotin binding sites on the beads including both an incubation and a washing step in the procedure. The controls would then show less RNA product in the activity tests than in the samples with polymerase bound beads.

6.2 Experimental

6.2.1 Procedure

2 × 10 μl streptavidin coated bead suspension were centrifuged down at 700 g, 5 min. in an eppendorf tube and the supernatant removed. The bead pellets were resuspended in 50 μl of washing buffer containing 10 mM NaCl, 40 mM Tris-HCl pH7.9, 6 mM $MgCl_2$, 10 mM DTT, 0.2 % BSA with and without 0.7 mM D-biotin. The final concentration of biotin binding sites on the beads were 0.7 mM. The suspensions were put at 4 °C for 30 min. The beads were centrifuged down at 700 g, 6 min and the supernatant removed. 100 μl washing buffer with and without biotin was added to each tube respectively and the beads resuspended, centrifuged again at 700 g, 6 min and the supernatant was removed. The beads were resuspended in 29 μl washing buffer (+/- biotin) and 0.86 μM T7 RNAP was added to give a final volume of 30 μl. The beads were put on a shaker in 4 °C, 1 h. The beads were then centrifuged down, the supernatant removed and the beads were washed with 3 × 200 μl washing buffer (+/- biotin) with centrifuge and removal of supernatant as mentioned above. The beads were resuspended in 10 μl reaction mixture as described in section 5.2.2 except the volume of RNAP was substituted with H_2O. As positive control a normal activity test was made as in section 5.2.2.

6.2.2 Results

In Figure 6.2 column 1 and 2 were loaded with beads incubated without and with biotin respectively and column 3 is the control. It is seen that the amount of template is less in the biotin control than in the sample. Due to this it cannot be determined whether the equally minor amount of RNA product is due to lack of template or, as it should, lack of bead bound T7 RNAPs. This experiment was repeated several times and the template band did not increase as hoped; a plausible explanation to the disappearing template could be that it stuck to the beads rendering them unavailable to transcription.

6.2.3 Increase of template concentration

To determine whether the small amount of RNA product in the biotin control was due to the decreased amount of available template and not due to blocked streptavidin binding sites as expected, the template concentration was increased from 2 ng/μl to 8 ng/μl and the experimental procedure in section 6.2 was repeated.

6.2.4 Results

Column 1 and 2 in Figure 6.3 is a repetition of column 1 and 2 in 6.2. Column 3 and 4 are similar to 1 and 2 respectively but with increased template concentration and they

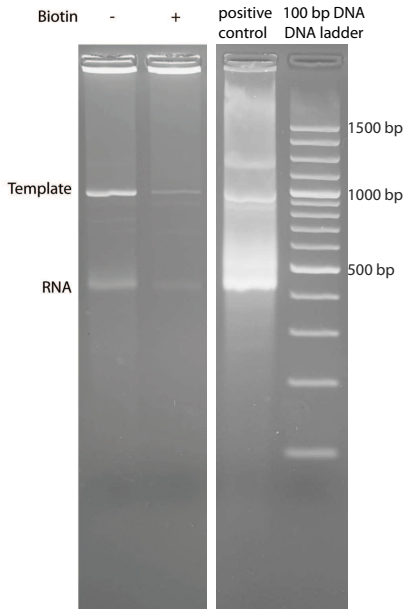

Figure 6.2: *Activity test of beads with and without biotin. From left to right: no biotin, with biotin, positive control, 100 bp DNA ladder. The control with biotin shows less template and RNA product than the sample without biotin.*

show that more templates result in increased RNA product in the samples both with and without biotin. The result confirms that the DNA sticks to the surfaces and to some extent inhibits transcription. In addition, as the activity is even higher in the biotin control it is possible that biotin increases nonspecific binding of the polymerase to the bead surface as well.

6.2.5 Alteration of salt concentration

In order to make the biotin control work, one possible way to circumvent nonspecific binding was to increase salt concentration to screen potential nonspecific binding sites. Activity tests of the T7 RNAP in various salt concentrations (results not shown) showed that $MgCl_2$ could not be increased to double concentration. This was possibly due to the fact that nucleotides can chelate Mg^{2+} ions[45] to form a stable complex where the nucleotide acts as electron donor and makes coordinate bonds with the positive metal ion. Hence they can be occupied in such a complex rather than being incorporated into new RNA, a situation that would result in transcription inhibition.[46] Therefore the Mg^{2+} concentration has to be carefully adjusted to the nucleotide concentration and accordingly, increased $MgCl_2$ requires increased rNTPs, which was not desirable. Increasing NaCl showed that the salt was tolerable up to about 50mM in an activity test. Once deciding on 50mM NaCl, further experiments showed that the T7 RNAP tolerated,

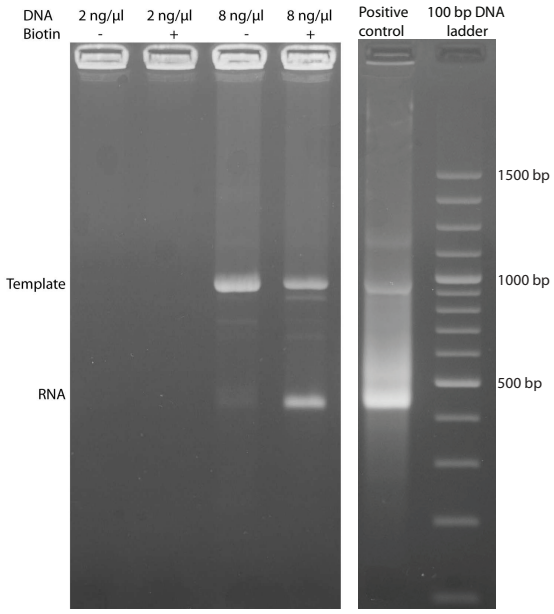

Figure 6.3: *Activity test of beads with and without biotin with extra template. Column 1 and 2 are a repetition of the previous test shown in 6.2 with 2 ng/µl DNA template. Column 3 and 4 are parallel samples of 1 and 2 but with 8 ng/µl template. These show more RNA product confirming not only that the template bind nonspecifically to the beads but the polymerase does so as well in the biotin control.*

but was somewhat affected, by Tris-HCl concentrations up to 150 mM above which it lost activity; therefore 100mM was chosen for the following tests with beads.

The samples were processed as described in 6.2 except the beads were preincubated with 0.1% BSA for 30 min in order to block possible nonspecific biotin binding sites, and the final concentration of T7 RNAP incubated with the beads was 2.58 μM.

6.2.6 Results

Columns 1–2 show activity without biotin and column 3–4 with biotin; column 2 and 4 have extra DNA template. The test shows that the polymerases generally produce more RNA product when extra DNA is present and consequently the conclusion is that nonspecific binding unfortunately was not circumvented and the RNA product deriving from the streptavidin bound RNAPs alone cannot be determined. Since the polymerase is active within a limited concentration range of the chosen buffer, other salts could be tested; yet biotin might well yield the same increased nonspecific binding.

To possibly make this setup work the concentration of T7 RNAP should be raised a 1000 fold to secure full quenching of biotin binding sites, achieving a higher amount

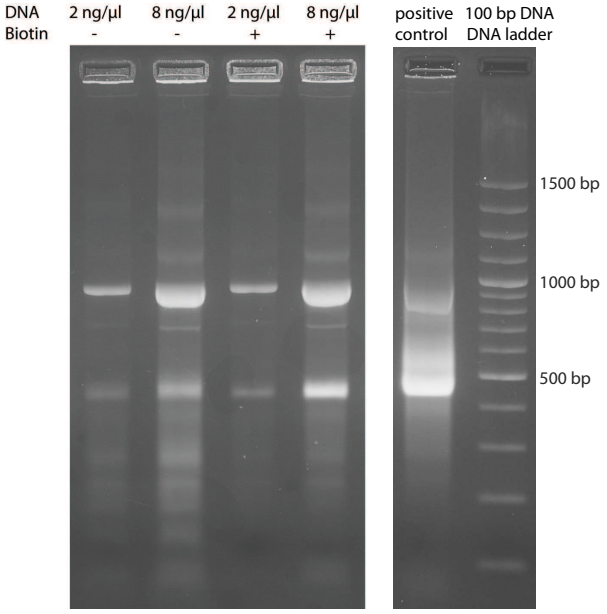

Figure 6.4: *Altered salt concentation did not change the tendency of the template and polymerase to nonspecefically bind to the beads. The test gives the same result as in 6.3 having more RNA product in the samples with extra template, column 2 and 4, particularly in the biotin control, column 4.*

of RNA product coming from bead bound RNAPs. This could help in disciminating RNA product coming from streptavidin bound RNAPs with that coming from nonspecific binding. However, such concentration of RNAP is not possible with the present purification procedure. All in all, the discrepancy between the RNAP concentration and the biotin binding capacity of the beads together with high nonspecific binding seems to be a reasonable explanation why this experiment failed.

Although the size of the beads and their easy visualisation incited their application in these experiments, the apparent problems in overcoming interactions between the biomolecules and the polystyrene surface, remained unsolved. Increasing the salt concentration did not change the behavior of nonspecific binding and consequently it was decided to turn to QDs as a probe for streptavidin bound polymerase activity.

Chapter 7

Ensemble studies of quantum dot bound T7 RNA polymerase

As the experiments on T7 RNAP binding to beads were not succesful, QDs were the next option in testing the activity of particle bound T7 RNAPs. As the size of a QD in the nm–range is comparable to macromolecules such as large proteins, it requires a different purification procedure than that given for the polystyrene beads presented in the previous chapter. The polystyrene beads could be separated from the surrounding medium and nonbound T7 RNAPs by centrifugation and removal of the supernatant, a procedure that relied on the easy visualisation of the bead suspension and pellet by eye; QDs however, required a different approach. This chapter introduces the initial experiments with QD migration in a gel and the considerations on the purification procedures gel filtration and affinity purification. Finally, the results of the purification procedure and the activity of the T7 RNAP conjugated to a QD is presented.

7.1 Electrophoretic mobility of QD:T7RNAP complexes

The QDs used in the present experiments are from Invitrogen and consist of a CdSe core of only a few thousand atoms, see Figure 7.1. The core is surrounded by a ZnS shell that improves the optical properties. The surface is coated with an amphiphilic polymer that makes the QDs soluble. Streptavidin molecules are conjugated to the amphiphilic polymer via a polyethylene glyco linker, PEG, that reduces nonspecific binding. The QDs are coated with 6-8 streptavidins (correspondance with Invitrogen).

Since the QDs are made of semiconductor material, a dipole moment can be induced in them, which could influence the migration of the particles in an electric field seen in the agarose gel Figure 5.3**b**. However, the migration of QDs in an electric field is also subjected to the chemical properties of their coating. For example, heavy coating

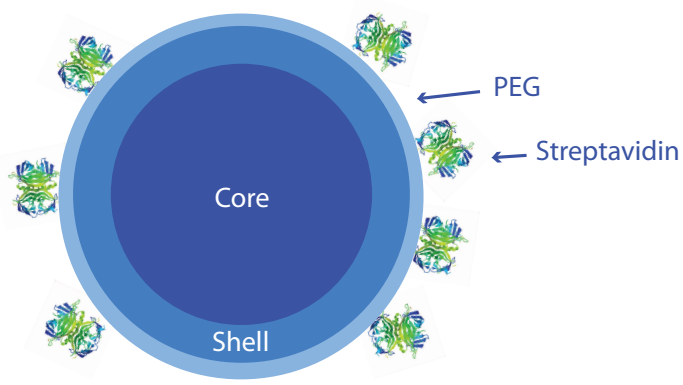

Figure 7.1: *Model of quantum dot illustrating the core, shell, PEG linker and streptavidin molecules. The relative size of QD and proteins is not drawn to scale.*

of QDs with PEG made the cojugated QDs move towards the cathode unlike the non-coated QDs;[47] also, QDs covalently coupled with dopamine molecules, a small aromatic compound, lose surface charges according to numbers of dopamine attached and consequently migrate slower.[48] Furthermore, QDs coated with BSA have been shown to slow migration towards the anode in a 4% agarose gel, which was attributed to both a lower charge and a greater diameter.[49]

The binding of T7 RNAPs alters the migration of the QDs through the agarose gel and separates them into two bands as seen in Figure 5.3**b** lane 5 and 10. Unlike the examples given above, T7 RNAP binding does not slow the QD diffusion through the gel matrix but increases it, which could be due to extra charges associated with the complex; this is discussed further below. Since the complex obtains a greater diameter upon binding compared to non-bound QDs, an increase of about 10 nm of 1 bound RNAP (about 20 nm when the RNAPs are bound on opposite sides of the QD), theoretically this should slow them through the gel. But as this does not happen, it is most likely that the complexes can diffuse through the gel independently of the size difference because of the large pore size in the agarose gel. The average pore size of a 2% agarose gel (close to the experimental 1.8%) was established with Atomic Force Microscopy, AFM, and found to be 364 nm with a distribution from 100 nm up to 600 nm.[50] This is much larger than the diameter of a QD with a T7 RNAP bound to it on each side, which would yield a total diameter of ≈34 nm. Agarose gels with concentrations 0.7-1% w/v are termed non-restrictive gels as the frictional retention of the gels are thought to be sufficiently low for the electrophoretic mobility to depend only on the net charge of the protein.[51]

As mentioned in section 3.1, a possible reason for the appearance of the second band is that the enzyme carries a total negative charge attributed to the Aspartate and Glutamate residues that contain negatively charged side chains. Because the aa residues Aspartate and Glutamate have pKs of 4.0 and 4.5 respectively and the theoretical isoelectric point of the T7 RNAP is pI=6.65[40] and the pH of running buffer is 8.53, the

Asp and Glu residues will be deprotonised. The charge of the RNAP might drag the QD:T7RNAP complex towards the anode during electrophoresis in spite of the larger size of the complex compared to the QD alone. A quantification of the total charge of the enzyme at the working pH is not simple, however, several calculator tools available on the internet predict the protein charge from the aa sequence at various pH; for the T7 RNAP at pH 8.53 these predictions range from -2 up to -14.[52] Since each QD according to Invitrogen can carry between 6-8 streptavidin molecules, each with four biotin binding sites, ideally 28 RNAPs can be attached, although steric hindrance comes into play. In the experiments presented below, approximately 3.6 RNAP bind to each QD, which based on the predicted charges above, gives a total charge in the range of -7.2 up to -50.

To further investigate this two gels were made, a 1.8 % and 1 % agarose gel with the latter expected to be nonrestrictive. The 1.8 % gel was loaded with 2.6 μM RNAP mixed with either 50 nM, 0.1 μM or 0.2 μM QDs; the 1 % gel was loaded with 0.1 μM QDs mixed with a decreasing amount of RNAPs, 2.6 μM, 1.3 μM, 0.26 μM, 0.13 μM, 86 nM and 26 nM. All samples were incubated in transcription buffer at 4 °C for 1 hour. Directly after incubation the complexes were run on the respective agarose gels. In addition, in both gels, controls with QDs were incubated likewise in transcription buffer but with no T7 RNAPs. An additional control on the 1 % gel was made with QDs in transcription buffer with 5 % glycerol and 8 mM imidazol, as these chemicals are present in the RNAP stock.

Figure 7.2 shows the resulting 1.8 % and 1 % gels. Column 1 in the 1.8 % gel shows that QDs alone migrate till about 1500 bp on the DNA ladder. Column 2 shows that the presence of T7 RNAP causes the QD band at 1500 bp to be less prominent and most of the complexes appear further down at approximately 1300 bp. Increasing the QD concentration in column 3 and 4 causes the QD band at 1500 bp to reappear again due to a surplus of QDs relative to T7 RNAPs in the sample. Column 1 and 2 in the 1 % gel show how the QD:T7RNAP band migrate longer than those in column 3-7. A comparison of column 7 and 8 show that addition of glycerol and imidazol to the QDs did not have any effect on QD migration. Column 1 in the 1 % gel is comparable to column 3 in the 1.8 % and shows similar behavior with most of the QDs appearing in the lower band. Possibly the broad band is due to heterogenecity in the number of bound RNAPs. At lower RNAP concentrations, 0.26 μM, 0.13 μM, 86 nM and 26 nM, the second band disappears. Generally the 1 % gel did not reveal any extra bands or resolve the bands better. What it did show was that the 1.8 % gel is more restrictive than the 1 % gel.

The charge effect might also explain why the template at high RNAP concentrations and favourable activity conditions in Figure 5.2 is found closer to the anode of the gel; in that case the polymerases are still associated with the DNA, and consequently drag the DNA molecule further down the gel due to the residing charges on the enzyme.

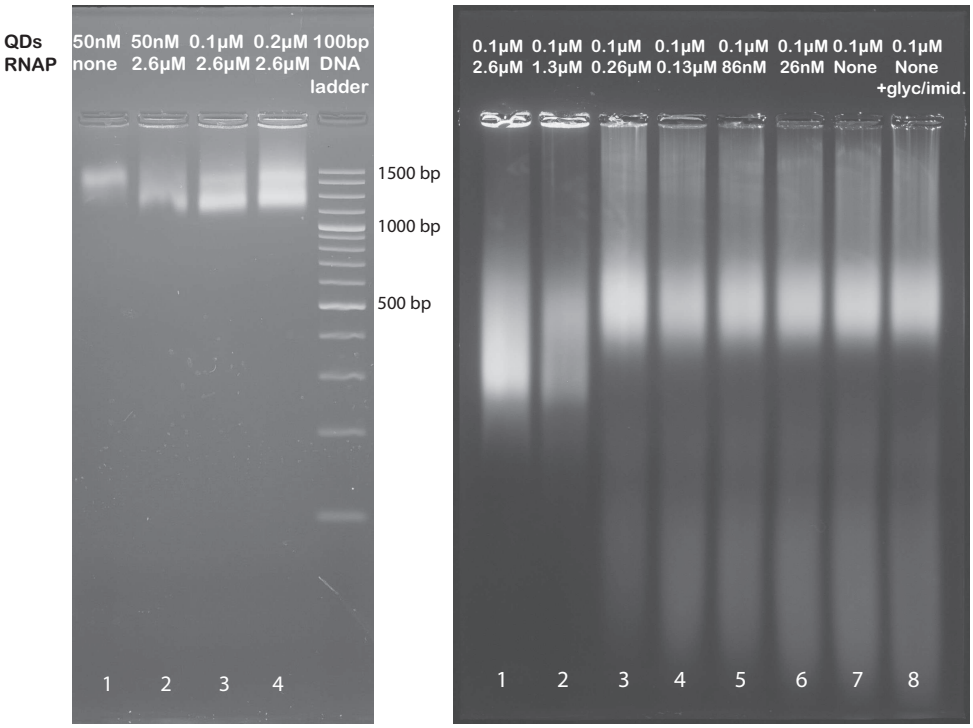

Figure 7.2: *QD bound polymerases cause QDs to separate on the agarose gel. The UV illumination causes the QDs to fluoresce. Left: 1.8 % agarose gel with varying QD concentration. Right: 1 % agarose gel with varying RNAP concentration. The QDs are incubated with 2.6 μM, 1.3 μM, 0.26 μM, 0.13 μM, 86 nM and 26 nM corresponding to lane 1-6 respectively. Lane 7 is QDs with no T7 RNAPs.*

7.2 Purification of QD:T7RNAP complexes

7.2.1 Considerations

Two options for purification of the QD:T7RNAP complexes were considered. The first option was to run the complex solution through an avidin resin in order to catch the surplus of free enzymes and then spin the QD:T7RNAP though a size separation filter that will exclude the avidin resin, see Figure 7.3. The advantage of this method is that the set up is easy and will take up little time to run; furthermore, the heavy QDs are expected to diffuse towards the bottom of the tubes when centrifuged. The presence of complexes and avidin capture of free enzymes is visualised indirectly with the RNA product in an activity test and since the amount of enzymes that are bound to QDs cannot be determined directly, it is presumably not as informative a method in this respect. However, lowering the RNAP concentration until no RNA product is seen in the activity tests of the avidin resin, the approximate QD:T7RNAP ratio maybe could be found. Alternatively, denaturation of the bound enzymes subsequently run on an

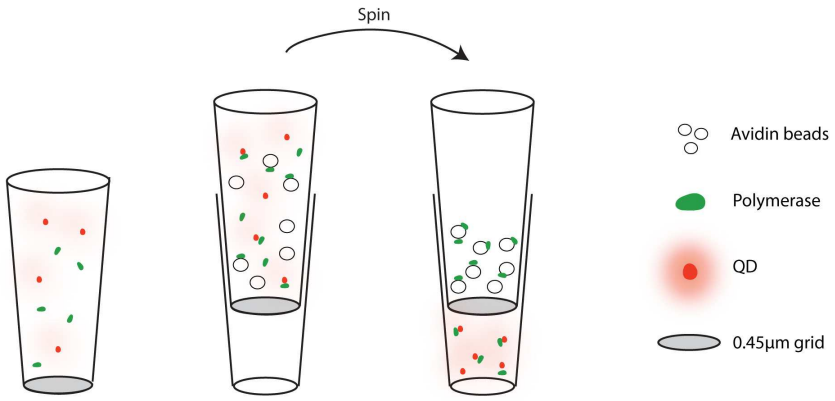

Figure 7.3: *Separation of complexes from free polymerases. Left: in the reaction tube the biotinylated T7 RNAPs (green dots) are mixed with streptavidin coated QDs (red dots) forming biotin-streptavidin bonds. Middle: the suspension is mixed with avidin coated beads (white dots) to capture the remaining free T7 RNAPs. Right: once the suspension is centrifuged on a 0.45 nm filter (grey plate) only the QD:T7RNAPs and free QDs are let through to the bottom.*

SDS-gel, might give some clue to the fraction of bound enzymes. Nevertheless, applying the avidin resin allows determination of whether or not the RNAP is active when it is bound to streptavidin.

The second option was gel filtration which has previously shown to separate free proteins from the QD bound ones.[53] Gel filtration sorts proteins according to their size through a matrix in a column at constant pressure. Proteins at different sizes are detected via their light absorbance and collected in small fractions. The advantage of gel purification is that the complexes and free proteins are visualised directly as distinctive absorption bands at different time points. Therefore, one can be sure to collect QD:T7RNAP complexes that are separate from non-bound enzymes. Also, a decrease in the absorbance of free enzymes could show the fraction of bound enzymes.

Unfortunately a drawback of both methods is the lack of discrimination of bare QDs and RNAP conjugated QDs: firstly, the physical properties of the QDs, such as the weight, are predominant over those of the enzyme in gel filtration, see for example Zhang *et al*;[53] secondly, using a 0.45 μm grid as size separation filter will let all QDs through whether bound or not since the total diameter of the streptavidin conjugated QD is much smaller. Nevertheless, the subsequent single molecule experiments do not necessarily require exclusion of non-conjugated QDs, because those that are bound, are expected to show qualities related to the RNAP, e.g., directed motion, stalling, etc. To save time the avidin resin procedure was chosen.

7.3 Experimental

7.3.1 Formation of QD:T7RNAP complexes

As the QDs are coated with 6-8 streptavidins the number of RNAPs bound to each QD can be controlled only by adjusting RNAP and QD concentrations and therefore relies on an average. As one streptavidin molecule has four biotin binding sites the QD can ideally conjugate about 28 RNAPs although steric hindrance has to be taken into consideration.

During the activity tests, the RNA product should not derive from free RNAPs; so in order to monitor this, controls undergoing the same procedure as the samples but containing no QDs, revealed the amount of free RNAPs binding to the avidin resin and the amount escaping the resin in the flowthrough. In this way the optimal working concentration was found within the chosen binding procedure and avidin resin volume. In addition a control with *wt* T7 RNAP was prepared to test if these stuck to the avidin resin.

In a final volume of 30 μl, final concentration of T7 RNAP of 4.3 μM was mixed with 10 mM DTT, transcription buffer and 0.33 μM QDs (streptavidin coated Qdot605, Invitrogen). The mixture was left at 4 °C, $1\frac{1}{2}$ hours for the streptavidin and biotin to bind. Parallel controls consisted of the same solutions including T7 RNAP but no QDs and 2 u/μl *wt* T7 RNAP. Additional controls were regular activity tests prepared as described in 5.2.2 with 1.3 μM Bio-T7RNAP and 2 u/μl *wt* T7 RNAP.

7.3.2 Purification and activity of QD:T7RNAP complexes

Preceeding spot tests of flowthroughs that were examined in a microscope, proved that none of the avidin resin passed the 0.45 μm filters.

20 μl 1×transcription buffer was added to the QD:T7RNAP and control solutions; the volume was increased to ensure that enough material was let through the filter for the subsequent activity test since part of the solution will be retained in the resin and filter. For each sample 25 μl avidin resin (Promega) was washed in 200 μl transcription buffer and centrifuged 500 g, 1 min, to remove the buffer, and the filters were moved to clean tubes. Each of the final 50 μl QD:T7RNAP mixture were transferred to the prepared avidin resins, which were gently resuspended and put on a shaker at 4 °C for 1 hour for the free RNAPs to bind the avidin resin. The avidin/QD:T7RNAP suspensions were filter centrifuged (Pierce, 0.45 μm pore size) at 350 g, 1 min, and the flowthroughs collected. The filters were transferred to clean tubes and the remaining avidin resins were each washed with 100 μl transcription buffer, centrifuged at 350 g, 1 min, to remove any QDs, QD:T7RNAPs and possible free RNAPs and they were finally resuspended in 10 μl transcription buffer.

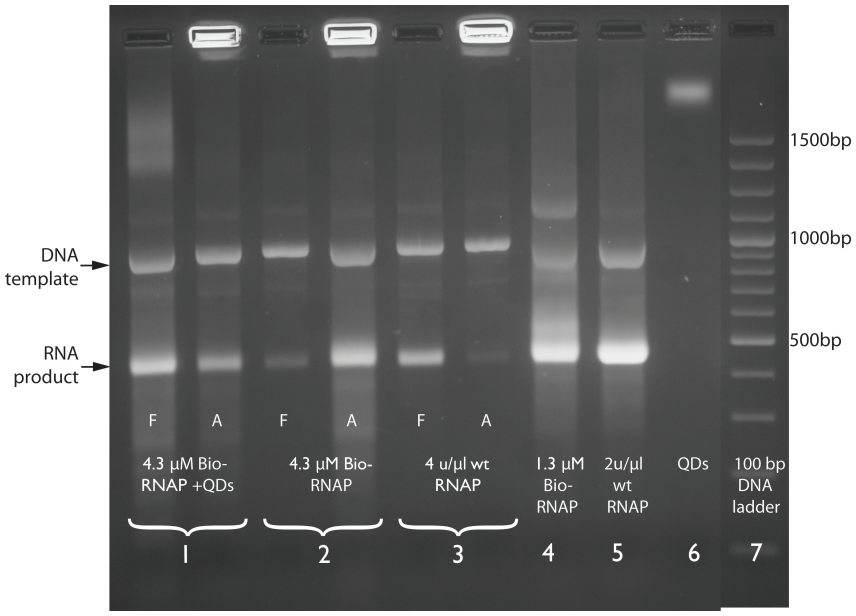

Figure 7.4: *Activity test of purified QD:T7RNAP complexes. Sample 1 shows tests of flowthrough (F) and avidin resin (A) containing the biotinylated T7 RNAPs and QDs of initial concentrations of respectively 4.3 μM and 0.33 μM, The controls: sample 2, which was similar to sample 1 but without QDs; sample 3, which contained a wt T7 RNAP that lacked the Bio-tag. This control showed that the majority of wt T7 RNAPs did not bind to the avidin resin but were collected in the flowthrough. Sample 4 and 5 were regular activity tests of respectively the 1.3 μM nonconjugated Bio-tagged T7 RNAP and the wt T7 RNAP. Sample 6 shows QDs alone and 7 is a 100 bp DNA ladder.*

6 μl of each collected flowthrough and of each final resuspended avidin resin were pulled for activity test at conditions described in Section 5.2.2.

7.4 Results

Sample 1 in Figure 7.4 has much RNA product in the flowthrough (F) but quite a lot appear in the avidin resin as well. Compared to flowthrough of the control, sample 2, a part of the RNA does derive from QD bound T7 RNAPs, however some is due to free T7 RNAPs. Sample 3 shows that most *wt* T7 RNAP passed the avidin resin and was collected in the flowthrough. This supports the fact that the conjugation of the Bio-T7RNAPs in sample 1 and 2 are mediated by the biotin-streptavidin bond only. This initial test showed that a QD:T7RNAP ratio of 1:13 (0.33μM:4.3μM) left a surplus of free RNAPs in the avidin resin. It also showed that the polymerase concentration was too high as RNA product from free T7 RNAP is seen in the flowthrough of the control. Therefore, the RNAP concentration was lowered in the following experiment. In order

to determine the approximate amount of RNAPs at which most were bound to QDs, three concentrations were tested: 4.3, 3.0 or 1.7 μM T7 RNAPs and the samples were prepared as described above.

Figure 7.5 shows the results of the activity test with samples of T7 RNAP binding concentrations of respectively 4.3, 3.0 and 1.7 μM: sample 1, 2 and 3 with QDs and the controls 4, 5 and 6 without QDs. The red arrow indicates the bands of RNA product coming from the flowthrough and avidin resin. Generally, sample 1, 2 and 3 and the controls C1, C2 and C3 demonstrate a fall in RNA product in accordance with the decrease in RNAP concentration. F and A denotes respectively the flowthrough and avidin resin.

Sample 1, 2 and 3 show that a great part of the QDs passed the 0.45 nm filter and did not stick to the avidin resin because they show up on the gel only in the flowthrough columns as two bands at 1500–1700 bp (blue arrow), compare the flowthrough with the avidin columns. The second band is due to RNAP binding consistent with the results presented above, compare with QDs alone in sample 5, yellow arrow.

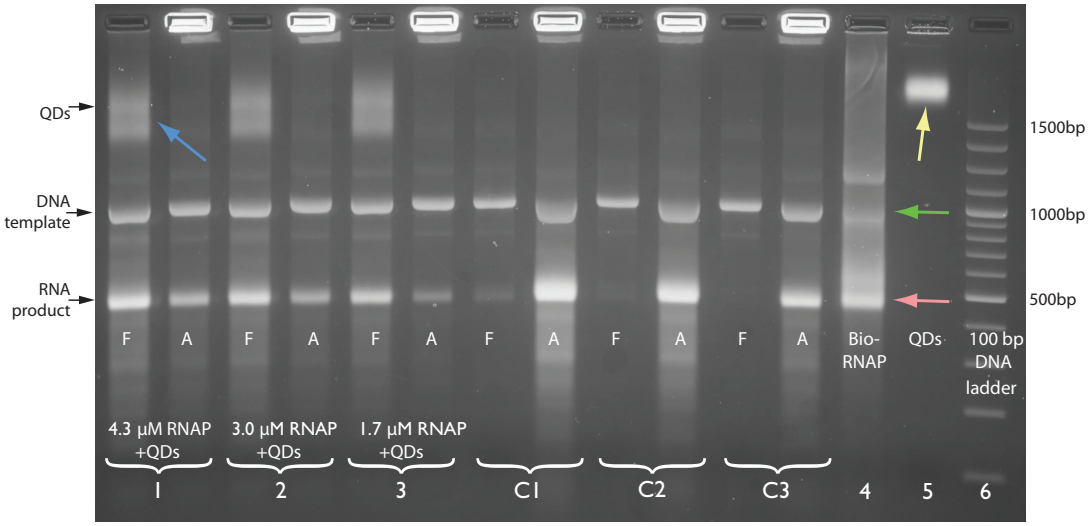

Figure 7.5: *Activity test of purified QD:T7RNAP complexes by avidin-binding of free RNAPs. Sample 1 - 3 and C1 - C3 each show the activity of 6 µl of the flow-through (F) and of the washed avidin resin (A). Red arrow indicates the RNA product. 0.3 µM QDs are used in the preliminary binding with 4.3, 3.0 and 1.7 µM biotinylated RNAP, respectively 1, 2 and 3 on the gel. C1, C2 and C3 are parallel controls of 1, 2 and 3 but with no QDs. Sample 4 shows the activity of free RNAP, 5 the QDs alone (yellow arrow) and 6 is a 100 bp DNA ladder.*

Most fortunately, a comparison of sample 3 with the control, C3, verifies that the RNA product present in the flowthrough of 3 primarily comes from QD bound T7 RNAPs. No RNA product and hence RNAPs is present in the flowthrough of sample C3, which means that the surplus of free T7 RNAPs are captured by the avidin. This fact indeed allows confirmation that the biotinylated T7 RNAPs maintain activity when they are bound to QDs.

A comparison of the RNA product of the flowthrough and avidin resin of sample 3, still shows a surplus of RNAPs in the avidin resin. In order to determine the fraction of surplus RNAPs, ImageJ Gel Analyser was applied for calculation of intensities of the bands, paying no heed to potential effects of either QD or agarose resin on RNAP activity. The analysis showed that 30% of the total amount of polymerases in sample 3 were surplus. Subtracting 30% from the initial RNAP concentration of 1.7 μM suggests that all RNAPs will bind to QDs in a solution with 1.19 μM of RNAPs to 0.33 μM QDs. Therefore a rough estimate of the polymerase:QD ratio in sample 3 is approximately 3.6:1. The estimate does not take into account the reasonable chance of losing a fraction of the QD:T7RNAP complexes and non-bound RNAPs during the final washing step of the avidin resin. Therefore, repeating the test with further reduction of the T7 RNAP concentration with RNA product in the flowthrough only, might yield a better basis for determining the ratio. However, the ratio is not far from that recently found by Mittal *et al*,[21] who measured the binding capacity of 605 nm streptavidin coated PEG QDs (Invitrogen) with biotin-4-fluorescein by monitoring the fluoresence quenching. They found a ratio of 2:1 (biotin:QD), which could be batch specific as they pointed out. Interestingly, their findings showed that a larger QD surface area did not necessarily increase the number of attached streptavidin molecules.

The degree of QD bound RNAPs could be enhanced by increasing incubation time and especially by letting the mixture stand at room temperature. Nevertheless, to minimise any enzyme degradation by proteases and possible denaturing, the RNAP was kept at 4 °C during handling.

The amount of RNA product in the flowthrough and avidin (F+A) resin of sample 3 should correspond to the RNA product in the control C3. They had the same T7 RNAP concentration and were subjected to the same procedure, the QDs excepted in the control. The intensities of the bands with RNA product in sample 3 (F+A) were quantified with ImageJ Gel Analyser. The bands with RNA product in C3 were likewise quantified and the two samples differed in intensity by 5% only, which supports the assumption that the T7 RNAP retained similar activity whether conjugated to QD or the avidin resin. A comparison of the relative intensities in Figure 7.4 of sample 1 (F+A) and sample 4, the nonconjugated T7 RNAP, with the relative initial T7 RNAP concentrations in the samples, shows that the conjugated T7RNAP lost 10% of its activity.

The activity test of QD bound T7 RNAPs is an indirect method of measuring the purity of complexes compared to gel purifiation. However, running the complexes through an avidin resin was easy and time saving and required little preparation. Most importantly,

the results showed that it is possible to functionalise the T7 RNAP with a QD and that the T7 RNAP preserves its activity while bound to a QD. A further interesting study would be to establish the enzyme kinetic parameters such as the turnover number, which would help to illuminate the effect of surface proximity on the T7 RNAP compared to parameters of free T7 RNAPs.

All in all, with the results presented in this chapter, the first aim of the project outlined in the introduction was reached, namely to verify the activity of T7 RNAPs bound to a particle. The next aim was to apply the single molecule techniques TPM and video microscopy to track QD:T7RNAPs on surface tethered DNA and demonstrate that the QD:T7RNAPs are active in a setup that requires somewhat different conditions. The remaining chapters will focus on these experiments.

Chapter 8

Tethered particle motion

This chapter summarises the initial TPM experiments conducted with beads. The application of beads was thought as a best introduction to TPM before turning to QDs as the object of molecular marker, partly because beads are readily visible in a bright field microscope due to their large size and partly because they do not require special visual techniques compared to the QDs. The applied beads are the same as those used in the work presented in chapter 6. The theory presented in chapter 3.4, mainly the definitions of the end-to-end displacement, r_{ee} and the root mean square deviation, RMSD, were taken into consideration during the process. This chapter begins with an explanation of how recordings of tethered beads were selected, before turning to the experimental procedure and the results.

8.0.1 Selection criteria

In order to select among many recordings of DNA tethered beads, which exhibited the properties of a random walk and showed no surface sticking, they were subjected to some selection criteria. Firstly, in order to estimate the magnitude of excursion of the DNA used in the following experiments equation 3.4 was used: for a 1336 nm DNA molecule with ξ=53 nm, r_{ee} was found to be 307 nm. However, this value is for the DNA alone. The observed (x,y) positions are those obtained from the centre of the bead and not from the DNA attachment point on the bead; bead attachment to DNA increases r_{ee} as earlier reported by Han *et al.*. They used a 892 nm long DNA and a bead with radius 245 nm, which resulted in a RMSD of about 325 nm.[54] Therefore, in the present experiments a larger r_{ee} is expected, but how large is not clear. Based on these considerations and on initial experiments it was reasonable that all calculated RMSDs of the experimental (x,y) positions have to fall within a certain minimum and maximum threshold, so as a start all RMSD values below 100 nm and above 600 nm were discarded.

Secondly, if the bead stuck to the surface at time intervals, which was seen as a sub-

stantial excursion decrease in the time traces of position, these were excluded from the analysis. This criterium did not employ mathematics in the analysis but the excursion traces were entirely evaluated by eye; for a mathematical approach, see Han *et al.*[54]

Thirdly, the symmetry of the (x,y)-scatter plot is important as the shape of it has to be circular and not elipsoid, which signifies a double DNA tethered bead. Other artefacts such as doughnut shapes, which exhibited symmetry on the scatter plot but where the bead excursions were situated entirely on a circle, were omitted from the data set. For symmetry determination of the scatter plot, a Matlab script was applied that set a threshold to the deviation of the plot from a circle. The mathematical approach was inspired by Han *et al*[54] and the script written by L Jauffred.[55]

8.1 Experimental setup

8.1.1 Chamber construction

Parafilm was cut and placed to form a 20-25 μl well on a 60×24 mm glass slide. A 50×24 mm glass slide was placed as lid. The chamber was heated for the parafilm to stick to the glass surfaces. 25 μl 20 μg/ml anti-digoxigenin in TE (10 mM Tris-HCl (pH 8), 1 mM EDTA) was flushed into the chamber and let stand at 4 °C overnight or at least 1 hour at 25 °C. Then 25 μl TE containing 0.2 % α-casein (TE/α-cas) was flushed through the chamber and incubated for 1 hour at 25 °C to block the glass surface. 25 μl 1 nM of DNA (stock 1) was flushed into the chamber and incubated for 1 hour at 4 °C for the digoxigenin-labelled end to bind to the anti-digoxigenin-coated surface. 5 μl bead suspension was washed with 20μl of 0.2 % α-casein in TE, centrifuged 2 min at 1500 g, the supernatant removed and the beads were resuspended in 30μl of TE/α-cas, which was flushed into the chamber. After 30 min the chamber was flushed with 150 μl TE/ α-cas to remove unbound beads and finally the chamber was sealed with vacuum grease. Controls were chambers processed similarly but without DNA. Finally, test samples contained DNA newly made from PCR (stock 2) where the DNA concentration was increased from 1 nM to at least 10 nM.

8.1.2 Image acquisition

The chamber was mounted on a stage and beads were selected on account of sufficient movement determined by eye and then recorded. The recordings were all made at room temperature on an inverted bright field Leica microscope using a 100× objective with numerical aperture of 1.4 and an immersion oil with n_e= 1.518, see Figure 8.1. Tethered beads were recorded with Para Sequencer 1.62, which gives the fps, the number of lost frames, the total number of frames and also saves the chosen object template as well as an image of the total tracked object path. The image resolution was either 72.72 nm/px or

44.79 nm/px if using a camera zoom. Image acquisition speed varied according to image size, however, with the zoom about 200 fps was attainable using image size 100×100 px. The image sequences were recorded as either tiff files or an AVI file.

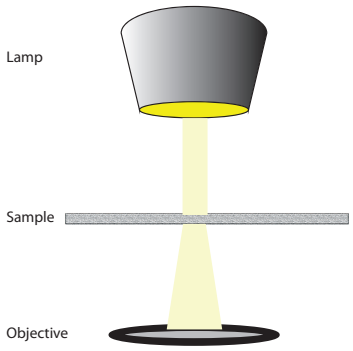

Figure 8.1: *Microscope setup: the sample is illuminated with light, which is scattered by the sample and some passes to the objective. The resulting image is defined by the contrast of reflected and transmitted light from the sample.*

8.1.3 Data processing

The images were analysed with the St. Andrews Tracker, StAT,[56] a LabView programme, which tracks the centre of an object of interest. The TPM results have not been corrected for drift, however the films were cut to 24 s sequences. A check of the drift of surface stuck beads (N=8) revealed that it changed RMSD for some measurements by a maximum of 4 nm.

The StAT programme output the x,y-coordinates of the object centre in a text file as two vectors, which were loaded in a Matlab programme that processed the data for statistics on the bead position. First the symmetry of (x,y) positions was checked using the criterium introduced above and those of non-circular shape were omitted. This criterium left out about 50% of the recordings. Next the data was processed in a second Matlab programme, written by M Anderson, which output the RMSD according to equations 3.5 and 3.6 for each recorded bead.

8.2 Results

Figure 8.2 shows an example of a scatter plot of the (x,y)-positions and the corresponding histogrammes of positions in the x and y direction respectively of a tethered bead that passed the selection criteria outlined above. The scatter plot has the desired circular shape and the x and y histogrammes are distributed around 0, which is ideally the tether attachment point. The obtained distributions were fitted to a Gaussian distribution, but

show a tendency to be assymetric. What causes this is not clear, but as pointed out earlier tethering of beads and the surface itself might influence the experimental data. The controls without DNA had much less beads that were tethered compared to the samples with DNA and hence it is clear that the DNA influences the amount of tethers. However, the control experiments revealed that particles could indeed be tethered even though no DNA was present, but possibly because of dirt or non-dissolved α-casein. Figure 8.3 shows the RMSD distribution of 126 measurements of which 22 are controls

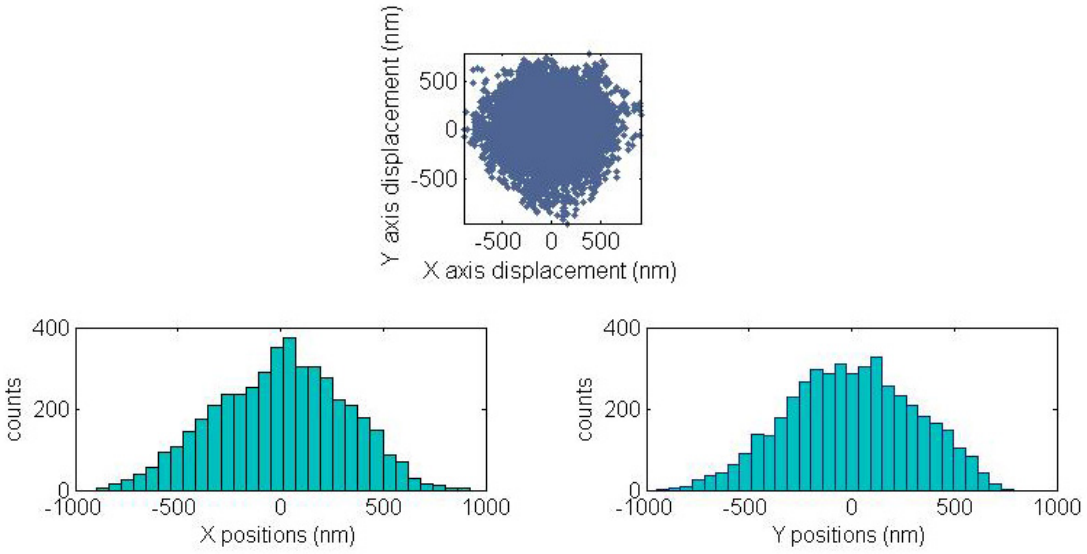

Figure 8.2: *Top: example of X,Y-scatter plot from DNA tethered bead, which has passed the selection criteria. Bottom: histogram of position distribution in the x (left) and y (right). The positions center around the mean at 0, which idealy corresponds to the tether point at the surface.*

(green). The RMSD distribution for DNA (stock 1) is shown in blue and that of stock 2 is shown in light blue. A total of 241 measurements were selected for analysis of which 52% passed the symmetry criterium. Almost none of the recorded beads had RMSD below 100 nm and none above 600 nm. The controls resemble the major part obtained from experiments with DNA tethers (blue); the mean of RMSD of DNA tethers is $RMSD_{dna}$ $\pm$std =(235 $\pm$59) nm and that of the control is $RMSD_c$ $\pm$std =(200 $\pm$53) nm. A Students T-test was applied to the two distributions and it showed a value of p=0.014 (t=2.49, d.f.112). This means that the error made by assuming two distinct distributions is about 1%, hence the controls are not the same as the samples. The 12 remaining measurements with RMSD values above 350 nm, corresponds to 5% of the total data set, most of these are from samples with newly synthesised DNA. The difference in RMSD values for the two DNA stocks might be due to different PCR procedures as the new DNA was not subjected to gel extraction, consequently, the stock might contain various impurities affecting the tethers.

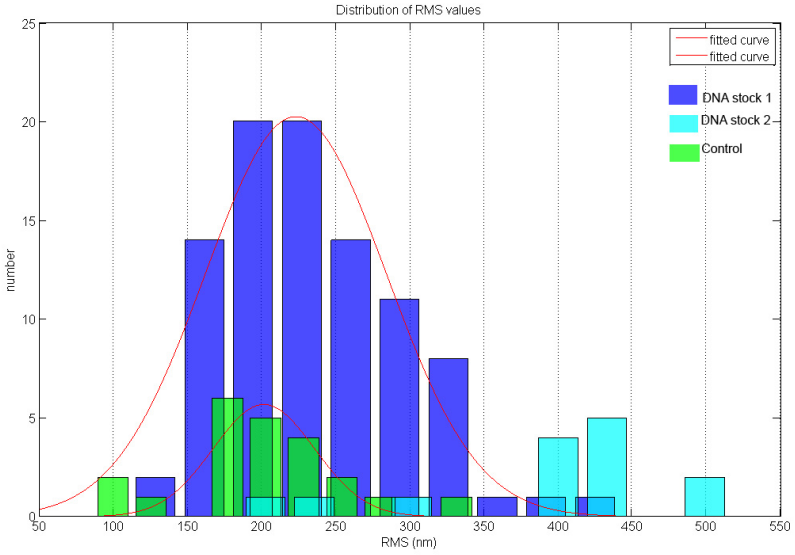

Figure 8.3: *Distributions of calculated root mean squares for data passing the selection criteria. Blue: RMS of measurements made with DNA (stock 1); green: controls without DNA; light blue: measurements with DNA of stock 2. The blue and green distributions are fitted to a Gaussian.*

The distribution of DNA tethered beads has a mean $RMSD_{dna}$ ±std =(235 ±59) nm, which is quite low compared to that obtained by Han *et al.* They calibrated TPM experiments with various sizes of DNA tethers and beads, for example, a DNA tether of 892 nm bound to a bead with radius=245 nm resulted in RMSD≈320 nm. In addition, Nelson *et al*[57] obtained RMSD≈360 nm (DNA length=1182 nm, bead radius=240 nm). The present setup with DNA tethers of 1336 nm and beads of radius=255 nm should result in a greater RMSD than that obtained by Han *et al.* The 1336 nm DNA was previously used for tethering QDs (radius=8 nm) by L Jauffred, who obtained 238 nm[58] actually exceeding the RMSD from the present experiment, which is inconsistent with the findings of Han *et al*, who showed that the measured RMSD grows as the bead size increases.

The effect of bead size on RMSD promts the application of smaller probes in TPM, for example, the QD. In this respect, the effect of bead size on DNA attached to a surface, is explored in a theoretical work by Segall *et al.*[59], who found an expression for the moment of a DNA molecule's excursion that shows a dependence on the ratio between the bead radius and the tether length, called the excursion number. This number is defined as:

$$N_R = \frac{R}{\sqrt{\frac{NL_k\xi}{3}}} \quad , \tag{8.1}$$

where R is the radius. It estimates two regimes with respectively molecule dominated motion, N_R<1, and bead dominated motion, N_R>1. The experiments presented here include beads with $N_{R,bead}$=1.66. Thus the bead size is expected to have some influence on the molecule conformations. Replacing the bead with a QD of R=8 nm, $N_{R,QD}$=0.052 and hence the QD has very little influence on the DNA conformations and these would resemble those of free DNA. Taking N_R into consideration, it is possible that attachment of a bead to DNA on a surface alter the DNA excursion. The effect of beads size on the DNA conformations and consequently also its effect on the biological system in focus is still a subject for studies, see, for example, Milstein *et al.*.[60]

The results presented here are inconclusive and more experiments are needed to settle on an RMSD value for the chosen setup. The use of a different DNA stock showed the sensitivity of the setup, so a lot more parameters need to be settled to render the data reliable. Nevertheless, the aim was to demonstrate the praxis of TPM and the next chapter introduces the first attempts to apply TPM on QD:T7RNAPs bound to DNA.

Chapter 9

Single molecule studies

In chapter 7 it was shown that the T7 RNAP retains activity when bound to a QD. Now the next challenge was the actual single molecule experiment presented in the introduction. However, previously, several attempts to monitor a transcribing T7 RNAP were made in vain. Therefore as a step in between the ensemble and single molecule experiment, a TPM experiment was suggested as a pendent to the experiments presented in chapter 7, which could enable the monitoring of many transcribing QD:T7RNAPs at one time, in order to easily get some average estimates and adjust working conditions accordingly. The T7 RNAP has to show activity under conditions that are different from those in the ensemble experiment. For example, the test chamber is made of glass coated with α-casein and glued together with parafilm and the T7 RNAP has to transcribe DNA that are fixed at one end. One disadvantage employing a TPM experiment is the problems that follow working close to a surface. The advantage however, is that the surface can be scanned easily for tethered QD:T7RNAPs. In the following sections two experiments are presented: one applying short DNA tethers and one applying long DNA tethers.

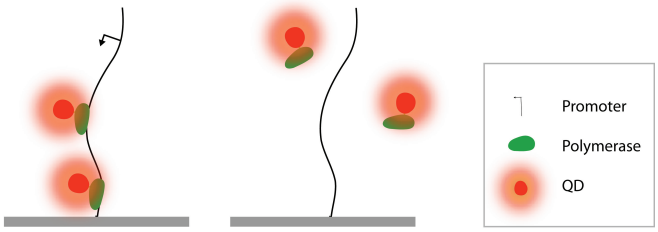

Figure 9.1: *Setup of single molecule assay with the short DNA. The DNA is bound to the surface (grey). Left: the QD:T7RNAP (red/geen) binds to the promoter (arrow) and accumulates on the DNA. Right: short DNA without a promoter resulting in no transcription.*

9.1 Experimental outline

The setup of the TPM experiment is shown in 9.1. The DNA that does not contain a terminator is bound at the 5′ end to the surface via an antidigoxigenin/digoxigenin bond, thereby positioning the promoter at the other end of the DNA to direct transcription towards the surface. The experiment relies on the presumption that the T7 RNAP will bind to the promoter and transcribe down the DNA till it meets the antidigoxigen and/or surface, which subsequently will make it stall. The stalled polymerase will then block the forward movement of upstream T7 RNAPs thus resulting in a queue up of T7 RNAPs on the DNA. Visualisation of the blockage of T7 RNAPs on the DNA was facilitated by fluorescence of the QD bound to each T7 RNAP, which increases as the queue of polymerases lengthen.

9.2 Considerations

It was decided that the experiment should be conducted with a short DNA tether in order to fix the QD:T7RNAP in a small volume. This would ensure that the QD fluoresence did not fall completely out of the focal plane due to fluctuations of the DNA; a QD bound at the end of a long DNA tether allows stronger fluctuation and hence the fluorescence would fall in and out of focus more easily. Regarding the transcription buffer, the single molecule experiments so far had not used spermidine because it had been shown to coil the DNA (communication with L Jauffred, F Czerwinski). However, tests presented in section 5.2.5 showed that spermidine greatly enhanced activity and therefore it was included in the following experiments. The initial TPM experiments established that α-casein and not BSA was preferable as coating of the chamber surface because BSA made the QDs stick to the surface. On the other hand, BSA was preferred as the blocking agent in the preparation of QD:T7RNAPs solutions in eppendorf tubes as the absence of BSA resulted in substantial loss of QDs.

9.3 Experimental

9.3.1 DNA construction

Two pieces of DNA, (A) ($\sim$ 670 bp) and (B) ($\sim$ 550 bp), respectively with and without the T7 promoter, were designed by S Sempsey from the plasmid pGEM4Z (Promega) using the primers:

(A), 5′-GGAATTGTGAGCGGATAACAATTTCACACA-3′,
(B), 5′-TATAGTGTCACCTAAATCCAATTCAC−3′.

In addition, for the opposite DNA strand to bind to a anti-digoxigenin-coated glass

surface, a digoxigenin-label was introduced to the DNA with the primer:

5′-Dig-CAAATAGGGGTTCCGCGCACATTTC-3′.

The DNA was produced using a standard PCR procedure and purified with GeneJET PCR purification kit (Fermentas).

9.3.2 Chamber construction

Two types chambers were prepared as descibed in section 8.1.1, except that the chambers were flushed with either 25 μl 1 nM of type (A) or (B) DNA and incubated for 30 min at 25 °C for the digoxigenin-labelled end of the DNA to bind to the anti-digoxigenin-coated surface. 25 μl 2 mg/ml BSA in transcription buffer was flushed through the chamber and let stand at 4 °C for 1 hour. Meanwhile, a stock of complexes were prepared in transcription buffer with 2.6 μM T7 RNAP and 0.1 μM QDs that was let stand at 4 °C at least 1 hour. 20 μl of 0.26 nM T7 RNAP/0.1 nM QDs in transcription buffer was flushed into the chamber that was mounted on the microscope stage and the surface was identified with fluorescence from surface stuck QDs. The stock complexes were diluted to 2.6 nM T7 RNAP and 1 nM QDs in transcription buffer with 2 mg/ml BSA, 2 mg/ml spermidine, 2 mM of each rNTP and 10 mM DTT and flushed into the chamber, which was sealed with vacuum grease.

9.3.3 Microscope setup & image aquisition

The chamber was placed in an inverted Leica microscope and examined using an 100× oil objective. To excite the QDs the sample was illuminated with 420 nm light from a mercury lamp, see Figure 9.2. To visualise the fluorescence coming from the QDs the light was filtered with a filter cube (see appendix 3) that allowed the 420 nm light to pass onto the sample but cut off the light to ensure that only the 605 nm fluorescence light from the QDs could pass back to the objective and EMCCD camera (Andor). Image sequences of 1000 frames were recorded with $\approx$ 5 f/s.

9.3.4 Intensity analysis

The Image files were analysed with the ImageJ programme Spottracker2D to perform tracking of the QDs and a custom made Matlab script previously written by L Jauffred. The following procedure was applied in order to observe any fluorescence increase during the recordings: intensity spots were identified and cut from the recorded image frame. Likewise, to correct for background noise, an area of the the imaged surface was identified without any intensity deriving from QD and was cropped similarly. A single image contained a number of pixels, each with a greyscale value that was loaded into Matlab as a matrix. The mean of all the pixel values of one image frame yielded the intensity

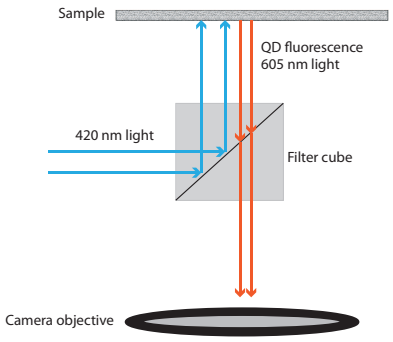

Figure 9.2: *The sample is irradiated with UV light to excite the QDs and the filter cube only allows the emmision light from the QDs to pass to the objective.*

of the image. This value was subtracted with the blacklevel value obtained from the background reference in the same way. The procedure was repeated for all image frames in the sequence and the intensity values for the entire sequence was plotted as a function of time.

9.3.5 Results

The experiments involving the short DNA did not reveal any difference in the intensity traces between the sample and the control (DNA without T7 promoter). Another problem was to discriminate between surface stuck QDs and those that were tethered. Subsequent experiments where the concentrations of complexes, DNA and nucleotides were altered, did not change the traces.

The presumption that intesity spots would occur and increase was not proved valid with the present DNA. The problem was to focus on a surface area without knowing how many, if any, tethers were present. To circumvent this problem DNA labelled with biotin at the free end would be able to bind a streptavidin coated QD. This would inevitably ease the quantification of available tethers on the surface before flushing in the complexes. In addition, the length of the DNA was altered from ≈ 250 nm to ≈ 1000 nm so that a tether was easily identified by its thermal fluctuations. The control was a parallel chamber that did not contain rNTPs, thus preventing transcription. Finally the chambers were to incubate at 37 °C to optimise transcription conditions. The setup is shown in Figure 9.3; the idea was that the polymerase would accumulate on the DNA during incubation of the samples with rNTPs whereas this would not happen on the control. Hence, the steady state of T7 RNAPs on the DNA could be visualised.

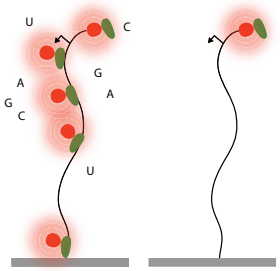

Figure 9.3: *Single molecule setup employing 3000 bp DNA. Left: the sample contains rNTPs which promote transcription and the QD:T7RNAPs accumulate on the DNA. Right: the control lacks rNTPs and as a consequence no transcription occurs and the complexes can only bind the biotin molecule at the end of the DNA via streptavidin on the QD.*

9.4 Change of DNA

9.4.1 Construction of long DNA

A 3250 bp piece of λ-DNA was inserted between the EcoRI and HindIII of the plasmid pGEM4Z previously. For PCR two primers were constructed labelled with biotin and digoxigen respectively to give a ∼3000 bp DNA:

5′-Bio-TGTGATGCTCGTCAGGGGGGCGGAGC-3′.

5′-Dig-TTCTCATGCTGAAAACGTGGTGTACCGGC-3′.

Premixed Platinum PCR Supermix High Fidelity (Invitrogen) was used for PCR. The DNA product was transferred to wells on a 1 % agarose gel in 1×PBE and run at 50V for 4 h. The 3000 bp bands were excised and the DNA purified with QIAquick Gel Extraction Kit giving ∼100 ng/μl.

The chambers were prepared as described above with the exception that the complexes were flushed into the chamber only once together with the reaction mixture of rNTPs, spermidine, DTT and BSA. For control a parallel chamber was made that contained the same DNA but no rNTPs. Before investigation of the chamber in the microscope the chambers were sealed with grease and put in a 37 °C incubator for 20 min. For some chambers the time interval was increased. This step was included to observe whether the complexes had lined up on the DNA which would facilitate recordings that reflected the maximum intensity possible from DNA accumulated QD:T7 RNAPs. Recordings of 1000 frames were performed.

9.4.2 Intensity analysis

In both the samples and the controls the brightest intensity spots were identified by eye. They were all tethered QDs that performed thermal fluctuations in and out of the focal plane. The image sequences were analysed with the Matlab script to output the intensity traces as described above. The maximum intensity of each trace was identified and cut out of the total image sequence. Sufficient image frames before and after the image containing the intensity maximum was included for analysis. The cut image sequence that included the maximum intensity value, was processed again as described above to find the intensity value of each image. The total intensity, denoted I, was the mean of the intensity value derived from each image in the sequence. The total intensity, I, was normalised to I_0, which was found similarly by processing intensity spots identified on the controls without rNTPs. These would assumably correspond to one QD bound to biotin at the end of the DNA. The intensity analysis was performed by L Jauffred.

9.4.3 Results

Result are shown in Figure 9.4. a) is an intensity histogram of I/I_0 of samples (red) and controls (green) and it shows that the intensity spots on the samples have significantly higher values than those on the controls. The higher intensity values are most likely due to the presence of the T7 promoter that allows several QD:T7RNAPs to accumulate on the DNA. The samples also contained spots with the same I/I_0 as the controls, which correspond to tethers having one QD at the free binding end of the DNA. b) and c) show the DNA tether with and without a promoter respectively. In b) two types of binding to the tether occur: a QD can form a streptavidin biotin bond at the end of the tether and the QD:T7RNAPs can bind to the T7 promoter and transcribe along the DNA. In c) the absence of the T7 promoter only allows a complex to bind to biotin via streptavidin on the QD. d) and e) are typical images of the the situations depicted in b) and c) respectively.

9.4.4 Discussion

There is a significant difference in the intensities obtained from the samples, which is an indication that the presence of nucleotides cause the T7 RNAP to bind and transcribe the DNA. In other words, this proves that the T7 RNAP retains activity under the conditions required for the single molecule experiments. More experiments are needed in order to establish whether the I/I_0 distribution accumulate around a mean value. It seems that a combination of longer DNA tethers and the rise in temperature of the samples to 37 °C caused the intensity increase. The experiments conducted with short DNA was also incubated at 37 °C but did not yield any intensity difference. This could indicate that longer DNA and hence a greater r_{ee}, see section 3.4, facilitates a greater volume for nonspecific DNA binding and hence for promoter search; another reason could be

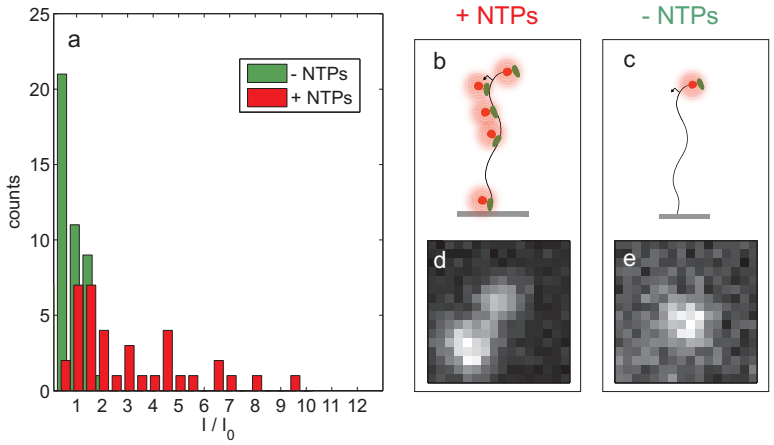

Figure 9.4: *Results of single molecule experiment with 3000 bp DNA. a) Histogram of sample intensities, I, (+rNTPs, red), normalised to control intensities, I_0, (-rNTPs, green). The sample values are markedly higher than those of the controls. The fluorescence spots on the control all show intensities that center around the value 1.*

that a part of the DNA is situated further above the glass surface compared to the short DNA making the occurence of surface/T7 RNAP interactions less likely, this, however is speculative only. The fact that temperature had a beneficial effect on the the T7 RNAP accumulation on the tethers is in agreement with the initial tests shown in Figure 5.3**a**. In fact, the samples were treated exactly the same way as those of the ensemble experiments in order to obtain the best conditions for activity including incubation at 37 °C, and thus this approach resulted in 'snapshot' of the steady state of T7 RNAPs on the DNA corresponding to the final situation depicted in Figure 9.4**b**.

The addition of spermidine, the increase of rNTP concentration and the temperature treatment, however, did have an effect on the fluorescence visualisation, as there was a time lag on the fluorescence appearance when the sample was placed under the mercury lamp, see Figure 9.5. This compromised the otherwise ease with which the surface could be scanned for tethers and it will also compromise future experiments with focus on the accumulation af T7 RNAPs on DNA over time and the tracing of the corresponding intensity increase. Therefore, further experiments have to be conducted to find a reasonable concentration and/or temperature at which possible chemical processes do not interfere with the fluorescence detection.

The knowledge gained from the ensemble experiments on the transcription buffer, the QD:T7RNAP formation and determination of concentration and activity, eased the way for better establishment of the conditions for the single molecule setup. The results of the single molecule experiment verified that the QD:T7RNAP is active in a setup that

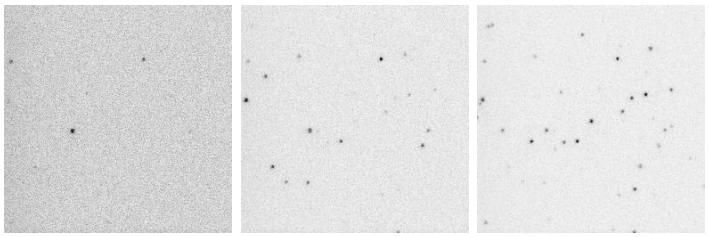

Figure 9.5: *example of the increase in fluorescence spots of image no. 1, 500 and 1000 recorded over ≈ 200 s. The greyscale has been inverted for ease of visulisation. Many fluorescence spots did not appear readily but showed up after some time of illumination. The spots in the area that had just been illuminated fluoresced immediately when illuminated again, whereas focusing on a new area just beside it did not, which gave rise to a visible 'edge' between the two areas.*

is different from the ensemble setup, especially taking the surface immobilised DNA into consideration. Although the results reflect the steady state of T7 RNAPs on DNA tether, the goal, which was visualisation of T7 RNAPs on a single DNA molecule, had been reached and the results motivate further experiments into the kinetics and DNA traffic of the T7 RNAP. An interesting experiment would be to add a flow to the setup descibed above after reaching steady state of T7 RNAP accumulation on the DNA. This would stretch the DNA and allow us to visualise the T7 RNAP distribution on the DNA molecule. Finally, the setup proposed in Figure 2.3 could be the next challenge in this project.

Chapter 10

Conclusion and perspective

This study has accomplished the first succesful results on the DNA traffic of the T7 RNAP. Establishment of the working conditions and activity tests of the QD:T7RNAP complex in the ensemble experiments were a prerequisite for the succesful single molecule experiments. The single molecule experiment verified that the QD:T7RNAP is also active in a different setup with surface immobilised DNA, which is essential for future single molecule studies of the T7 RNAP. Thus the first and partly the second aim of this project has been fulfilled. All in all, the work presented here gives evidence that functionalisation of a T7 RNAP with a QD via a streptavidin–biotin bond is possible and that the T7 RNAP retains activity under conditions required for both an ensemble and a single molecule experiment, a fact that has not been shown before.

The next challenge in this project is to probe T7 RNAP elongation with the setup illustrated in Figure 2.3. The setup is one possible approach but other options are equally sound and available in our laboratory, for example, a flow chamber, where DNA is immobilised at one end to the surface and aligns with the flow of the surrounding medium to stretch the DNA, or the replacement of the micropipette with a second optical tweezers. This work motivates interesting future experiments on T7 RNAP collisions and on DNA traffic that involves the T7 RNAP interactions with other proteins associated with the DNA, such as roadblocks, inhibitors and other types of enzymes such as the DNA polymerase and the ribosome. DNA traffic is an important topic in our understanding of fundamental processes in biology such as gene regulation; it underlines the neccesity for the development of functional labelled proteins in order to probe their interactions on the single molecule level -interactions that could eventually enrich our knowledge in this field.

Chapter 11

Appendices

11.1 Appendix 1, Purification of T7 RNA polymerase

A cell colony was grown in 4ml LB with 100μg/ml chloramphenicol and ampicillin overnight at 37 °C and transferred to 400 ml TB + 8 ml 20 % glucose + 100 μg/ml chloramphenicol and ampicillin and grown until OD=1. At this point 6 ml 100 mM IPTG/50 μM biotin was added and cells incubated for 3 hours at 30 °C. Cells were centrifuged down at 6000 g and resuspended in 4.6 ml 20 mM Tris-HCl, pH 8. 1 ml 20 mg/ml lysozyme was added and the cells were put on ice for 30 min. 5 ml lysis buffer (20 mM Tris-HCl, pH 8.0, 1 M NaCl, 0.1 % Tween20, 5 mM imidazol, 5 mM β-mecaptoethanol) was added and the cells were put on ice for additional 30 min and were then centrifuged 45 min at 15000 g and the supernatant collected. 1 ml washed Ni^{2+}-agarose resin suspended in lysis buffer was transferred to the lysate and the mix was put in 4 °C 1 hour and afterwards transferred to a column (Micro-Bio-spin chromatography columns, Bio-rad) at 4 °C. The Ni^{2+}-agarose resin was washed with 3× 0.7 ml washing buffer (20 mM Tris-HCl, pH 8.0, 0.5 M NaCl, 0.05% Tween20, 5 mM imidazol, 5 mM β-mecaptoethanol) and finally the bio-T7RNAPs were eluted with washing buffer containing 80 mM imidazol. The enzymes were stored in 50 % glycerol with 10 mM DTT.

11.2 Appendix 2, Article for publication

Specific binding of quantum dots to active T7 RNA polymerases

Mette Eriksen [‖†] Liselotte Jauffred [‖†] Peter Horvath,[‡] Michael A. Sørensen,[¶] Szabolcs Semsey,[†] and Lene Broeng Oddershede[*,†]

The Niels Bohr Institute, University of Copenhagen, Denmark, ELTE Budapest, Hungary, and BioCenter, University of Copenhagen, Denmark

[‖]Contributed equally
[‖]Contributed equally
[†]The Niels Bohr Institute, University of Copenhagen, Denmark
[‡]ELTE Budapest, Hungary
[¶]BioCenter, University of Copenhagen, Denmark

Abstract

The bacteriophage T7 RNA polymerase consists of a single polypeptide chain and can start *in vitro* transcription from a short promoter sequence. The simplicity of the T7 transcription system causes a versatile usage: It is used for high production of proteins in *in vitro* transcription and translation and it is also a very potent system to explore fundamental parameters in biological systems. These advantages of the T7 RNA polymerase makes it a prominent candidate for single molecule studies. To perform single molecule studies of the T7 RNA polymerase, it is crucial to monitor an individual T7 RNA polymerase, e.g., through a fluorescent signal. To this end, we designed an assay where quantum dots were specifically conjugated to T7 RNA polymerases. The labeling was mediated through an *in vivo* biotinylation of a his-tagged T7 RNA polymerase and subsequent binding of streptavidin-coated quantum dots. The quantum dot labeled T7 RNA polymerases could easily be purified from the reactants and they retained activity while bound to quantum dots. As proof of concept we monitored individual quantum dot labeled T7 RNAPs transcribing a surface-attached DNA tether.

INTRODUCTION

The enzyme that catalyzes transcription of genes is the RNA polymerase (RNAP). Transcription initiates at a promoter sequence with high RNAP-promoter affinity and continues until a termination sequence. Therefore, the RNAP shall balance two tasks: A stable binding to the DNA in order to transcribe the gene and the ability to disengage rather fast at the termination site. Proteins and other co-factors can inhibit or recruit RNAPs to DNA, thus regulating the initiation process. This process is highly complex involving many parts of the cellular machinery and recent single molecule experiments have been quite successful in unraveling the action of individual parts of this complex machinery (*1–4*).

Several families of RNAPs exist, e.g., the bacterial, the eukaryotic, the archaic, and the viral. Though the majority of reported single molecule experiments have been carried out using the bacterial *E. coli* RNAPs, other families are also of interest and have distinct properties. The viral

T7 RNA polymerase is a single subunit RNAP (98 kDa) (*5*) characterized by extreme promoter-specificity (*6*) and a very low error rate (*7*). The T7 family of RNAPs is structurally and evolutionary distinct from the multi-subunit family of RNAPs. T7 RNAP allows specific high-level transcription and expression of cloned genes (*8*), therefore, it is a key enzyme in the production of recombinant proteins, and also in several *in vitro* molecular biology applications (*9*, *10*). Such applications include generation of large quantities of capped or uncapped RNA transcripts for translation, synthesis of tRNA, rRNA, RNA virus genomes, ribozymes, microarray targets (*11*), production of substrates for RNA splicing (*12*), RNA secondary structure, antisense RNA, and RNA-protein interaction studies. The T7 RNAP is suitable for homogenous radioactive or non-radioactive labeling of single stranded RNA and it plays an important role in technologies based on RNA and DNA hybridization (*13*). A tight regulation of T7 RNAP expression is possible and T7 expression systems are therefore used for the production of otherwise deleterious protein products (*14*).

A wide variety of single molecule assays are designed to study the diffusive or directed translocation of molecular motors (*3*, *15*). In order to visualize or manipulate the individual motor, it is typically specifically attached to a fluorescent probe or a dielectric particle. An effective conjugation, which does not alter the activity of the enzyme, is absolutely essential in order to obtain trustworthy results. Due to their high quantum yield and large photostability (*16–19*) colloidal quantum dots (QDs) are a particularly good choice as labels for molecular motors. QDs have been used, e.g., to track the motility of individual receptors in a cell membrane (*20*), to track individual bacteriophages infecting bacteria (*21*), and to monitor individual proteins diffusing on DNA (*22*, *23*). Individual colloidal QDs can even be optically manipulated (*24*) and excited by the trapping laser through two-photon absorption (*25*), thus enabling both visualization and manipulation through specific attachment of a single QD. For these reasons, it is highly desirable to devise a method to specifically attach QDs to individual molecular motors. QDs can be taken up by living cells (*26*) and are non-toxic when encapsulated. Hence, they also have potential for *in vivo* studies of, e.g., the action of molecular motors.

Here, we show how to specifically label individual T7 RNAPs by QDs through a biotin-streptavidin bond and we show that the QD-functionalized T7 RNAP complex (QD:T7RNAP) retains activity. Previously, activity was proven of a QD-labeled *E. coli* RNAP (*27*), however, to our knowledge this is the first report of QD labeling of viral T7 RNAPs that retain activity after QD marking. The activity of the QD:T7RNAP is proven both in an ensemble assay and in a single molecule assay where QD:T7RNAP bind and elongate along short dsDNA tethers anchored to a surface. The accumulation of QD:T7RNAPs on DNA was investigated with wide-field fluorescence microscopy and an ultra-sensitive camera.

EXPERIMENTAL PROCEDURES

Protein purification and activity test

***In vivo* biotinylation and purification of T7 RNAP.** Our construct was based on plasmid pBH161 which was a generous gift from William T. McAllister, Department of Biochemistry, University of New Hampshire. Plasmid pBH161 encodes a T7 RNAP His-tagged N-terminally (*28*). We further tagged the enzyme N-terminally with a 15aa sequence, GLDIFEAQKIEWH, referred to as a Bio-tag, which was recognized by biotin ligase and biotinylated at a single lysine *in vivo* (*29*), Figure 1 gives an overview of the construction. The DNA sequence encoding the Bio-tag was synthesized by PCR using three primers:

5′-ATCACCATGGGTAGCAGCGGCCTGAACGACATCTTCGAAGCTCAGAAAA-3′.

5′-ATCTTCGAAGCTCAGAAAATTGAATGGCACGGCAGCTCTCATCATCATCATCATCATAG-3′.

5′-ATAGCTCGAGCATATGAGAACCGCGCGGCACCAGACCACTGCTATGATGATGATGATGATGAG-3′.

The synthesized DNA fragment was digested by XhoI and NcoI and inserted between the XhoI

and NcoI sites in pBH161 upstream of the sequence encoding the His-tag; the resulting plasmid was denoted pBioT7. Bio-His-tagged T7 RNAP was expressed in the *E. coli* strain BL21Star (Invitrogen) containing the plasmids pBioT7 and pBirA (Avidity). Enzymes were purified from the lysate using Ni^{2+}-agarose beads (Qiagen) and eluted with 80 mM imidazol.

Verification of activity of biotinylated T7 RNAPs. After the *in vivo* biotinylation of the T7 RNAP we tested that it was still active. The reaction mixture contained 2 ng/μl 1,000 bp DNA template with T7 promoter and terminator, transcription buffer (40 mM Tris-HCl pH 7.9, 6 mM $MgCl_2$, 10 mM NaCl), 2 mM spermidine, 10 mM DTT, 2 mM of each rNTP, 2 units/μl RNasin, and 2.6 μM Bio-T7 RNAP. The reaction mixture was incubated at 37 °C for 1 hour before running the agarose gel. The control protein (Phage 16-3 repressor, C16-3) was not biotinylated.

Quantification of biotinylation. To quantify the amount of biotinylated T7 RNAPs purified biotinylated T7 RNAPs were mixed with SoftLink^{TM}Soft Release Avidin Resin (Promega) and allowed to bind for 1 hour at room temperature. The mixture was loaded on Poly-Prep®Chromatography Columns (Bio-Rad) and the flow-through was collected. The column was washed with 10 bed volumes of buffer (20 mM Tris-HCl pH 7.9, 0.5 M NaCl, 0.05% (w/v) Tween 20). Samples of the flow-through, the washed fraction, and the matrix-bound fractions were loaded on a 4-12% NuPAGE gel (Invitrogen) along with a molecular weight marker (SeeBlue Plus2, Invitrogen). After electrophoresis the gel was stained with Coomassie Brilliant Blue.

Formation of QD:T7RNAP complexes. The *in vivo* biotinylated T7 RNAPs were attached to QDs in the following manner: In a final volume of 30 μl the biotinylated T7 RNAP solutions with final concentrations of either 4.3, 3.0 or 1.7 μM were mixed with 10 mM DTT, transcription buffer (40 mM Tris-HCl (pH 7.9), 6 mM $MgCl_2$, 10 mM NaCl), and 0.3 μM streptavidin-coated QDs (Qdot605, Invitrogen). The mixture was left at 4 °C for 1 1/2 hour allowing the streptavidin-biotin bond to form. Parallel controls consisted of the same solution with T7 RNAPs but without QDs present.

Purification of QD:T7RNAP complexes. In order to purify the QD:T7RNAP complexes 20 μl transcription buffer was added to the QD:T7RNAP and control solutions. Each of the final 50 μl

reactions were transferred to a 25 μl solution of pre-washed and centrifuged avidin resin. The resin was re-suspended and put on a shaker at 4 °C for 1 hour. The avidin and QD:RNAP suspensions were filter-centrifuged (pore size 0.45 μm, Pierce), only allowing the QD:T7RNAP and the free QDs to be in the flow-through which was collected for an activity test. This procedure is depicted in Figure 2. The avidin resins were washed with 100 μl transcription buffer and re-suspended in 10 μl transcription buffer and also collected for an activity test.

Activity of QD:T7RNAP complexes and avidin-bound RNAPs. Activity tests were performed of both the flow-through containing QD:T7RNAP complexes and of the washed avidin resin containing biotinylated T7 RNAPs bound to the avidin resin. The reaction mixture (10 μl) contained 2 ng/μl, 1,000 bp DNA template with a T7 promoter, transcription buffer, 2 mM spermidine, 10 mM DTT, 2 mM of each rNTP, 2 units/μl RNasin, and 6 μl of collected QD:T7RNAP solution. The reaction mixture was incubated at 37 °C for 1 hour before loading on the agarose gel. The two controls consisted of 1.3 μM biotinylated T7 RNAPs in the reaction mixture and 0.1 μM QDs in the reaction mixture.

As each QD is coated with 6-8 streptavidins (Invitrogen) the average number of T7 RNAPs bound to each QD can be controlled by adjusting RNAP and QD concentrations. The RNA product of the activity test should not derive from free RNAPs. In order to find the amount of RNA product originating from free RNAPs, controls undergoing the same procedure as the samples but with no QDs, revealed the amount of free RNAPs escaping the avidin resin in the flow-through. In this way the concentrations of T7 RNAPs and QDs yielding optimal working conditions (an absolute minimum of free RNAPs) were found.

Single molecule assay

DNA construct. A 3,250 bp piece of λ-DNA was synthesized by PCR using the primers:

5′ -TTTTGAATTCAAAAAACCCCTCAAGACCCGTTTA GAGGCCCCAAGGGGTTCTCATGCT-GAAAACGTGGTG TACCGGC-3′.

5′-TTTTTTAAGCTTGGACCTATCTGCCCGTTCGTCCC GTCGTT-3′.

This DNA piece was inserted between the EcoRI and HindIII of the plasmid pGEM4Z (Promega). Using this plasmid pLJP1 as a template, a $\sim 3,000$ bp DNA was constructed with biotin and digoxigen labels at the ends using the following primers:

5′-Bio-TGTGATGCTCGTCAGGGGGGCGGAGC-3′.

5′-Dig-TTCTCATGCTGAAAACGTGGTGTACCGGC-3′.

The DNA product was purified with QIAquick Gel Extraction Kit. At $\sim$ 500 bp from the biotinylated end, the DNA construct had a T7 promoter. There was no terminator site present.

Sample chambers. A perfusion chamber was made by placing parafilm forming a 20-25 μl well on a 60×24 mm glass slide and adding a 50×24 mm glass slide as lid. The chamber was heated such that the parafilm melted to the glass surfaces. To coat the surface with anti-digoxigenin 20 μg/ml anti-digoxigenin in TE (10 mM Tris-HCl (pH 8), 1 mM EDTA) was flushed into the chamber and left at 4 °C overnight or at least 1 hour at 25 °C. To minimize unspecific bindings to the glass surface transcription buffer containing 2 mg/ml α–casein was flushed through the chamber and incubated for 1 hour at 25 °C. 10 nM of the DNA solution was flushed into the chamber and incubated for 30 minutes at 25 °C such that the digoxigenin-labeled end of the DNA tether could bind to the anti-digoxigenin-coated surface. 2 mg/ml α–casein in transcription buffer was flushed into the chamber and left at 25 °C for 30 min. Finally, QD:T7RNAP complexes (2.6 nM RNAP and 1 nM QDs) in transcription buffer with 2 mg/ml BSA, 2 mg/ml spermidine, 2 mM of each rNTP, and 10 mM DTT were flushed into the chamber and the chamber was sealed with vacuum grease. The controls were processed similarly but without rNTPs in the transcription buffer.

Visualization. The samples were investigated using an inverted Leica microscope. A mercury lamp was focused with an oil immersion objective (Leica HCX PL APO 100× NA=1.4 oil, ∞ CS). To image the light emitted from the 605 nm QD we used a custom made filter cube (Leica HQ420/40x+1064, z440/1065rpc, HQ605/40m-2p) which allowed the 420 nm light from the

mercury lamp to be reflected up to the sample and only allowed the emitted 605 nm light to be transmitted to the EMCCD camera (Ixon, Andor) (*24*, *25*). The images were analyzed with ImageJ and custom made Matlab routines. In addition, we performed centroid tracking of the tethered QDs using the ImageJ tracking routine Spottracker2D (*30*).

RESULTS

Quantification of biotinylation

The amount of biotinylated T7 RNAPs was quantified using an avidin-coated resin. The protein gel in Figure 3 shows that very little protein is present in the flow-through and none in the washing buffer, hence, almost all T7 RNAPs were biotinylated. Based on the relative intensities, we estimated that 95-99% of the T7 RNAPs were biotinylated. The very high activity of the biotinylated T7 RNAPs is verified by the strong band at the expected weight of the product in lane 4 of Figure 4 (red arrow).

Activity of ensembles of QD:T7RNAP complexes

The activities of the QD:T7RNAP complexes and the corresponding controls are shown in Figure 4. The RNA products (red arrow) from the flow-through (F) and avidin resin (A) are shown for QD:T7RNAP concentrations of 4.3, 3.0, and 1.7 μM in lanes marked 1, 2, and 3, respectively. The corresponding controls, without QDs, are shown in lanes marked C1, C2, and C3. It is clear from lanes 1, 2, and 3 that the majority of the QDs passed the 0.45 nm filter and showed up on the gel in the F columns as two distinct bands (blue arrow) at 1500–1700 bp as earlier reported (*31*). Interestingly, the QDs with T7 RNAPs attached migrate further than the QD alone, to see this compare lane 5 (yellow arrow) to lanes F1, F2, or F3 (blue arrow). This is probably due to the fact that the net charge of the T7 RNAP at pH 8.5 (pH of the agarose gel) is -5 and therefore the QD:T7RNAP complex migrates faster towards the anode during electrophoresis than the free

QDs. The agarose gel pore size was relatively large in comparison to the size of the approximately spherical QD:T7RNAP complex. Hence, the fact that one or possibly more charged T7 RNAPs are attached, and thereby cause the complex to move faster in the field, have larger influence on the overall migration than the incremental increase in effective diameter (*32*).

A comparison, e.g., of lanes 3 with their controls, C3, verifies that the RNA product present in the F3 originated from QD:T7RNAP complexes only, since no RNA product is present in the flow-through of C3. As the surplus of free RNAPs is efficiently captured by the avidin resin, we conclude that the T7 RNAP is indeed active when bound to a QD. Our activity test of QD-bound RNAPs is an indirect method of measuring the purity of complexes compared to gel purification (*33*). However, running the complexes through an avidin resin is still reliable, time saving, and requires very little preparation.

QDs are only present in the flow-through (F) of lanes 1, 2 and 3, confirming that the majority of the QDs passed the filter and did not stick to the avidin resin. On the basis of the intensities of the bands originating from the RNA products of F and A we estimated a ratio 3-4:1 of RNAPs to QDs. This ratio is in accordance with a recent report on biotin binding to the same type of QDs (*34*).

Activity of individual QD:T7RNAP complexes on DNA tethers

As the QD:T7RNAP complex has a large potential for single molecule investigations we also tested its activity in a typical single molecule assay. The experiment and a control were conducted as sketched in Figure 5 b and Figure 5 c, respectively, utilizing a $\sim$3,000 bp DNA tether. The DNA tether was biotinylated at one end, had a T7 promoter 500 bp from the biotinylated site, and was attached to a coverslip at the other end. For the experiment (Figure 5 b) QD:T7RNAP complexes as well as streptavidin-coated QDs were flushed into the chamber together with the required NTPs. Individual QD:T7RNAP complexes thus attached at the promoter site and started transcription along the DNA tether. As there was no transcription termination sequence in the DNA the QD:T7RNAP complexes were prone to accumulation on the DNA tether close to the glass

surface. In addition, on most tethers a streptavidin-coated QD attached to the biotinylated end of the DNA tether, hence, overall, there was the option of multiple QDs on the tethers simultaneously. For the control (Figure 5 c) no NTPs were present and, hence, it was unlikely that any QD:T7RNAP complexes would attach to the promoter or start elongating. The only fluorescent signal expected from the control was that originating from a streptavidin-coated QD attached to the biotinylated end of the DNA tether.

In the experiments with the elongating QD:T7RNAP complexes (+NTP) we saw significantly more intense spots on the surface than in the control experiment (-NTP). Probably each originating from a single DNA tether with multiple QDs attached. A typical EMCCD image of the assay where multiple QDs are expected (+NTP) is shown in Figure 5 d. A typical EMCCD image from the control (-NTP) is shown in Figure 5 e. As the DNA tether itself performed thermal fluctuations in and out of the focal volume and the QD also exhibited blinking, the resulting intensity time series (with total length $\sim$ 200 s) have significant intensity fluctuations. In the analysis we used the window of 20 frames ($\sim$ 5 s) of each time series around the maximum intensity. The average intensity, I, of the window was normalized to the intensity average of a time series originating from the control (-NTP), I_0. The measured values of I/I_0 both for the experiment (red bars) and for the control (green bars) are plotted in Figure 5 a. The intensity distribution of the spots of the +NTP experiment is significantly higher and broader than the intensity distribution of the -NTP control. This verifies that in the presence of nucleotides QD:T7RNAP complexes did attach to the promoter and accumulated on the DNA tether. Hence, the QD:T7RNAP complexes are indeed active. On average it appeared that each DNA tether with multiple QDs attached had at approximately 5 QDs attached at a concentration of 200 nM T7 RNAPs.

DISCUSSION

The ensemble experiments showed that the the viral T7 RNAP could easily be efficiently biotinylated while retaining activity (*23*, *35*). In addition we showed that upon attachment of a

streptavidin-coated QD the QD:T7RNAP complex retains activity. In particular, we showed how to purify QD:T7RNAPs from a solution of un-bound RNAPs. As the conjugation and purification assays utilized were simple and still highly efficient, the devised procedure is recommendable for attachment and purification of QDs to T7 RNAPs.

In the single molecule assay the DNA tether was biotinylated at the free end, thus allowing a streptavidin-coated QD to attach to this end. In the control no NTPs were present. Hence, as the T7 RNAP requires the initiating nucleotide (GTP) for specific binding and protection of the T7 promoter from DNaseI digestion, it is likely that the QD at the end of the tether is the only QD affiliated with the DNA tether of the control. This was verified by the experiments (data shown in Figure 5 a). When the initiating nucleotide is absent, the enzyme randomly binds DNA with lower affinity (*36*).

The type of single molecule assay utilized in the present investigation is often termed the tethered particle method (TPM) and relies on DNA anchorage to a surface and some probe particle attached to the tether whose thermal fluctuations can be monitored. This type of assay has been widely used in literature, e.g., in the study of DNA-bound proteins (*37–39*). In our experiments the observed thermal fluctuations of a QD attached to the DNA in the control experiments were consistent with the length of the DNA tether (3,000 bp) and the size of the QD (13 nm (*25*)) (*40*, *41*). As the length from the promoter to the anchor point of the DNA tether was $\sim 100\times$ the length of an elongating complex there was space for several QD:T7RNAP complexes. The fact that we on average found 5 QD:T7RNAP complexes attached implies that typically the QD:T7RNAP complexes occupied at most 20 % of the DNA.

In comparison to the *E. coli* RNAP the viral T7 RNAP is relatively simple as it only consists of a single polypeptide chain and has a short promoter. The simplicity of the T7 RNAP as well as its high efficiency has paved the way for high production of specific protein products (*10*). Anyhow, only few single molecule investigations of the T7 RNAP exist in comparison to the detailed knowledge obtained on the single molecule level concerning the fundamental properties (e.g., transcription velocity, stalling force, pausing events, backtracking) of *E. coli* RNAP. We find the T7

RNAP an interesting enzyme and our results showed that it is indeed possible to conjugate a QD to a T7 RNAP while retaining its activity. This, along with our single molecule proof of concept experiment utilizing tethered particle motion, paves the way for single molecule investigations of the T7 RNAP and of the viral transcription machinery in general.

Acknowledgement

ME and LJ contributed equally. We acknowledge support from Jesper Tholstrup. The work was financed through the University of Copenhagen Excellence Program.

References

(1) Yin, H.; Wang, M.; Svoboda, K.; Landick, R.; Block, S.; Gelles, J. Transcription against an applied force. *Science* **1995**, *270*, 1653–1657.

(2) Wang, M.; Schnitzer, M.; Yin, H.; Landick, R.; Gelles, J.; Block, S. Force and velocity measured for single molecules of RNA polymerase. *Science* **1998**, *282*, 902–907.

(3) Bai, L.; Santangelo, T. J.; Wang, M. D. Single-molecule analysis of RNA polymerase transcription. *Ann. Rev. Biophys. Biomol. Struct.* **2006**, *35*, 343–360.

(4) Abbondanzieri, E. A.; Greenleaf, W. J.; Shaevitz, J. W.; Landick, R.; Block, S. M. Direct observation of base-pair stepping by RNA polymerase. *Nature* **2005**, *438*, 460 – 465.

(5) Stahl, S.; Zinn, K. Nucleotide sequence of the cloned gene for bacteriophage T7 RNA polymerase. *J. Mol. Biol.* **1981**, *148*, 481–485.

(6) Brown, J.; Klement, J.; McAllister, W. Sequences of three promoters for the bacteriophage SP6 RNA polymerase. *Nucleic Acids Res.* **1986**, *14*, 3521–3526.

(7) Brakmann, S.; Grzeszik, S. An error-prone T7 RNA polymerase mutant generated by directed evolution. *Chembiochem.* **2001**, *2*, 212–219.

(8) Studier, F.; Moffatt, B. Use of bacteriophage T7 RNA polymerase to direct selective high-level expression of cloned genes. *J. Mol. Biol.* **1986**, *189*, 113–130.

(9) Terpe, K. Overview of bacterial expression systems for heterologous protein production: from molecular and biochemical fundamentals to commercial systems. *Appl. Microbiol. Biotechnol.* **2006**, *72*, 211–222.

(10) Iskakova, M.; Szaflarski, W.; Dreyfus, M.; Remme, J.; Nierhaus, K. Troubleshooting coupled in vitro transcription-translation system dreived from Escherichia coli cells: synthesis of high-yield fully active proteins. *Nucleic Acids Res.* **2006**, *34*, e135–(1–9).

(11) Lockhart, D.; Dong, H.; Byrne, M.; Follettie, M.; Gallo, M.; Chee, M.; Mittmann, M.; Wang, C.; Kobayashi, M.; Horton, H.; Brown, E. Expression monitoring by hybridization to high-density oligonucleotide arrays. *Nature Biotechnol.* **1996**, *13*, 1675–1680.

(12) Krainer, A.; Maniatis, T.; Ruskin, B.; Green, M. Normal and mutant human beta-globin pre-mRNAs are faithfully and efficiently spliced in vitro. *Cell* **1984**, *36*, 993–1005.

(13) Zinn, K.; DiMaio, D.; Maniatis, T. Identification of two distinct regulatory regions adjacent to the human beta-interferon gene. *Cell* **1984**, *34*, 865–879.

(14) Wagner, S.; Klepsch, M.; Schlegel, S.; Appel, A.; Draheim, R.; Tarry, M.; Hogbom, M.; van Wijk, K.; Slotboom, D.; Persson, J.; de Gier, J.-W. Tuning Escherichia coli for membrane protein overexpression. *Proc. Nat. Acad. Science* **2008**, *105*, 14371–14376.

(15) Greenleaf, W. J.; Woodside, M. T.; Block, S. M. High-resolution, single-molecule measurements of biomolecular motion. *Ann. Rev. Biophys. Biomol. Struct.* **2007**, *36*, 171–190.

(16) Chan, W. C. W.; Nie, S. M. Quantum dot bioconjugates for ultrasensitive nonisotopic detection. *Science* **1998**, *281*, 2016–2018.

(17) Michalet, X.; Pinaud, F.; Lacoste, T. D.; Dahan, M.; Bruchez, M. P.; Alivisatos, A. P.;

Weiss, S. Properties of fluorescent semiconductor nanocrystals and their application to biological labeling. *Single Mol.* **2001**, *2*, 261–276.

(18) Michalet, X.; Pinaud, F.; Bentolila, L.; Tsay, J.; Doose, S.; Li, J.; Sundaresan, G.; Wu, A.; Gambhir, S.; Weiss, S. Quantum dots for live cells, in vivo imaging, and diagnostics. *Science* **2005**, *307*, 538–544.

(19) Larson, D.; Zipfel, W.; Williams, R.; Clark, S.; Bruchez, M.; Wise, F.; Webb, W. Water-soluble quantum dots for multiphoton fluorescence imaging in vivo. *Science* **2003**, *300*, 1434–1436.

(20) Dahan, M.; Levi, S.; Luccardini, C.; Rostaing, P.; Riveau, B.; Triller, A. Diffusion dynamics of glycine receptors revealed by single quantum dot tracking. *Science* **2003**, *302*, 442–445.

(21) Edgar, R.; Rokney, A.; Feeney, M.; Semsey, S.; Kessel, M.; Goldberg, M.; Adhya, S. Bacteriophage injection is targeted to cellularl poles. *Mol. Mocrobiol.* **2008**, *68*, 1107–1116.

(22) Biebricher, A.; Wende, W.; Escude, C.; Pingoud, A.; Desbiolles, P. Tracking of single quantum dot labeled EcoRV sliding along DNA manipulated by double optical tweezers. *Biophys. J.* **2009**, *96*, L50–L52.

(23) Ebenstein, Y.; Gassman, N.; Kim, S.; Antelman, J.; Kim, Y.; Ho, S.; Samuel, R.; Michalet, X.; Weiss, S. Lighting up individual DNA binding proteins with quantum dots. *Nano Lett.* **2009**, *9*, 1598–1603.

(24) Jauffred, L.; Richardson, A. C.; Oddershede, L. B. Three-dimensional optical control of individual quantum dots. *Nano Lett.* **2008**, *8*, 3376–3380.

(25) Jauffred, L.; Oddershede, L. Two-photon quantum dot excitation during optical trapping. *Nano Lett.* **2010**, *10*, 1927–1930.

(26) Marin, S.; Pujals, S.; Giralt, E.; Merkoci, A. Electochemical investigation of cellular uptake

of quantum dots decorated with a proline-rich cell penetrating peptide. *Bioconjugate Chem.* **2011**, *22*, 180–185.

(27) Finkelstein, I. J.; Visnapuu, M.-L.; Greene, E. C. Single-molecule imaging reveals mechanisms of protein disruption by a DNA translocase. *Nature* **2010**, *1*, 1–5.

(28) He, B.; Rong, M.; Lyakhov, D.; Gartenstein, H.; Diaz, G.; Castagna, R.; McAllister, W.; Durbin, R. Rapid mutagenesis and purification of phage RNA polymerases. *Protein Expres. and Purif.* **1997**, *9*, 142–151.

(29) Beckett, D.; Kovaleva, E.; Schatz, P. A minimal peptide substrate in biotin holoenzyme synthetase-catalyzed biotinylation. *Protein Sci.* **1999**, *8*, 921–929.

(30) Sage, D.; Neumann, F.; Hediger, F.; Gasser, S.; Unser, M. Automatic tracking of individual fluorescence particles: Application to the study of chromosome dynamics. *IEEE Transac. Image Proc.* **2005**, *14*, 1372–1383.

(31) Buecking, W.; Massadeh, S.; Merkulov, A.; Xu, S.; Nann, T. Electrophoretic properties of BSA-coated quantum dots. *Anal. Bioanal. Chem.* **2010**, *396*, 1087–1094.

(32) Clarke, S.; Hollman, C.; Aldaye, F.; J.L, N. Effect of ligand density on the spectral, physical, and biological characteristics of CdSe/ZnS quantum dots. *Bioconjugate Chem.* **2008**, *19*, 562–568.

(33) Zhang, H.; Zeng, X.; Li, Q.; Gaillard-Kelly, M.; Wagner, C. R.; Yee, D. Fluorescent tumour imaging of type I IGF receptor in vivo: comparison of antibody-conjugated quantum dots and small-molecule fluorophore. *Brit. J. Cancer* **2009**, *101*, 71–79.

(34) Mittal, R.; Bruchez, M. Biotin-4-fluorescein based fluorescence quencing assay for determination of biotin binding capacity of streptavidin conjugated quantum dots. *Bioconjugate Chem.* **2011**, *22*, 362–368.

(35) Thomen, P.; Lopez, P.; Bockelmann, U.; Guillerez, J.; Dreyfus, M.; Heslot, F. T7 RNA polymerase studied by force measurements varying cofactor concentration. *Biophys. J.* **2008**, *95*, 2423–2433.

(36) Basu, S.; Maitra, U. Specific binding of monomeric bacteriophage T3 and T7 RNA polymerases to their respective cognate promoters requires the initiatin ribonucleoside triphosphate (GTP). *J. Mol. Biol.* **1986**, *190*, 425–437.

(37) Tolic-Nørrelykke, S. F.; Rasmussen, M. B.; Pavone, F. S.; Berg-Sørensen, K.; Oddershede, L. B. Stepwise bending of DNA by a single TATA-box binding protein. *Biophys. J.* **2006**, *90*, 3694–3703.

(38) Lia, G.; Semsey, S.; Lewis, D.; Adhya, S.; Bensimon, D.; Dunlap, D.; Finzi, L. The antiparallel loops ingal DNA. *Nucleic Acids Res.* **2008**, *36*, 4204–4210.

(39) Beausang, J. F.; Zurla, C.; Manzo, C.; Dunlap, D.; Finzi, L.; Nelson, P. C. DNA looping kinetics analyzed using diffusive hidden Markov model. *Biophys. J.* **2007**, *92*, L64–L66.

(40) Segall, D.; Nelson, P.; Phillips, R. Volume-exclusion effects in tethered-particle experiments: Bead size matters. *Phys. Rev. Lett.* **2006**, *96*.

(41) Jauffred, L.; Sletmoen, M.; Czerwinski, F.; Oddershede, L. Quantum dots as handles for optical manipulation. *Proc. SPIE* **2010**, *7762*, 776226.

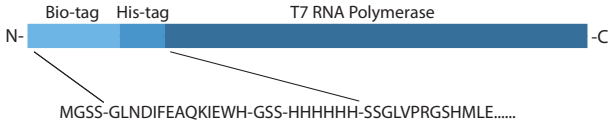

Figure 1: N-terminal amino acid sequence of the biotinylated T7 RNAP. The N-terminal part of the enzyme begins with a 15aa sequence recognized by biotin ligase. Then follows a 3aa spacer and the His_6-tag whereupon the aa sequence of the T7 RNAP begins.

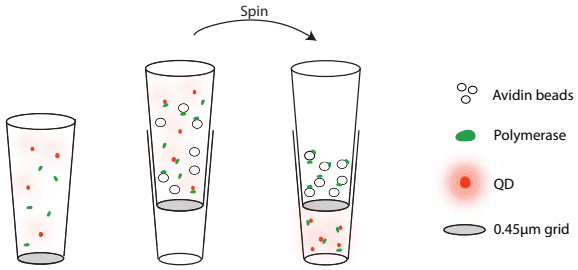

Figure 2: Separation of QD:T7RNAP complexes from free RNAPs. The biotinylated RNAPs are mixed with streptavidin-coated QDs forming biotin-streptavidin bonds. The suspension is mixed with avidin resin to capture the remaining free RNAPs. Once the suspension is centrifuged on a 0.45 μm filter only the QD:T7RNAP complexes and free QDs reach the bottom.

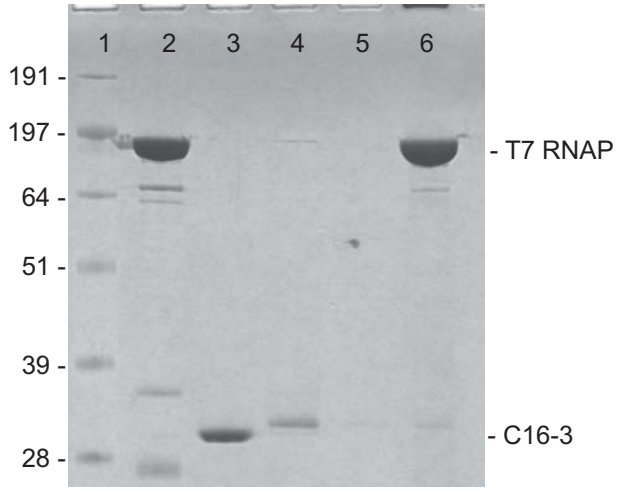

Figure 3: Efficiency of *in vivo* biotinylation of T7 RNAP. T7 RNAP is compared to a control protein which is not biotinylated (C16-3). Purified *in vivo* biotinylated T7 RNAP (lane 2) and C16-3 (lane 3) were mixed with avidin resin and filtered. A very little amount of RNAP is found in the flow-through (lane 4) and none is found when washing the avidin resin (lane 5). Lane 6 was loaded with the proteins bound to the avidin resin; this is where the large majority of T7 RNAPs are found. Lane 1 is a weight marker.

.

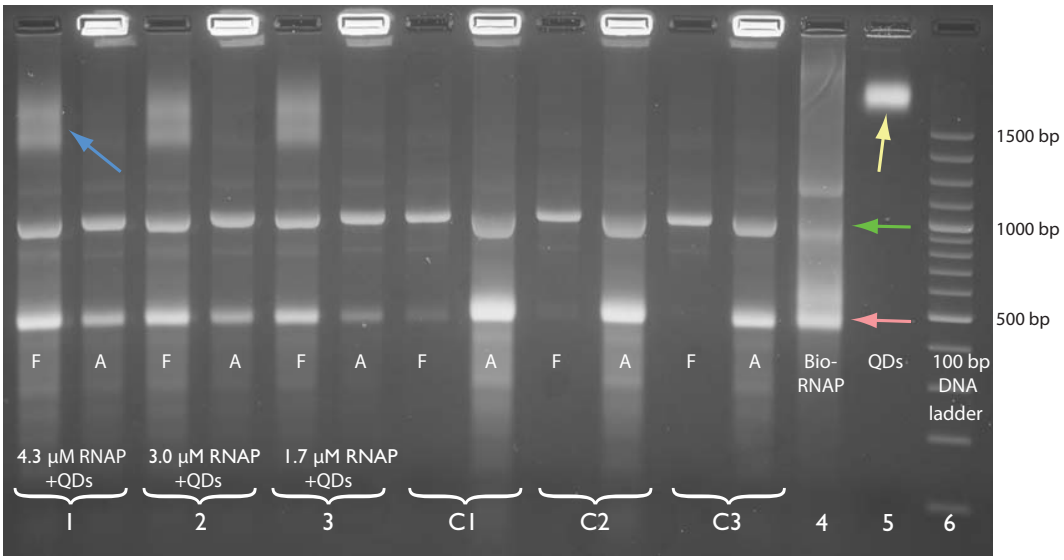

Figure 4: Activity test of purified QD:T7RNAP complexes and the corresponding controls. Lanes 1 - 3 and C1 - C3 each show the activity of 6 μl of the flow-through (F) and of the washed avidin resin (A). 0.3 μM QDs are used in the preliminary binding with 4.3, 3.0, and 1.7 μM biotinylated RNAP, these are shown in lanes 1, 2, and 3 on the gel. C1, C2, and C3 are parallel controls of, respectively, but without QDs. Lane 4 shows the activity of free biotinylated RNAP, lane 5 the QDs alone, and lane 6 is a 100 bp DNA ladder. The red arrow marks the RNA product, blue arrow marks QD:T7RNAP bands, and yellow arrow marks bands of free QDs.

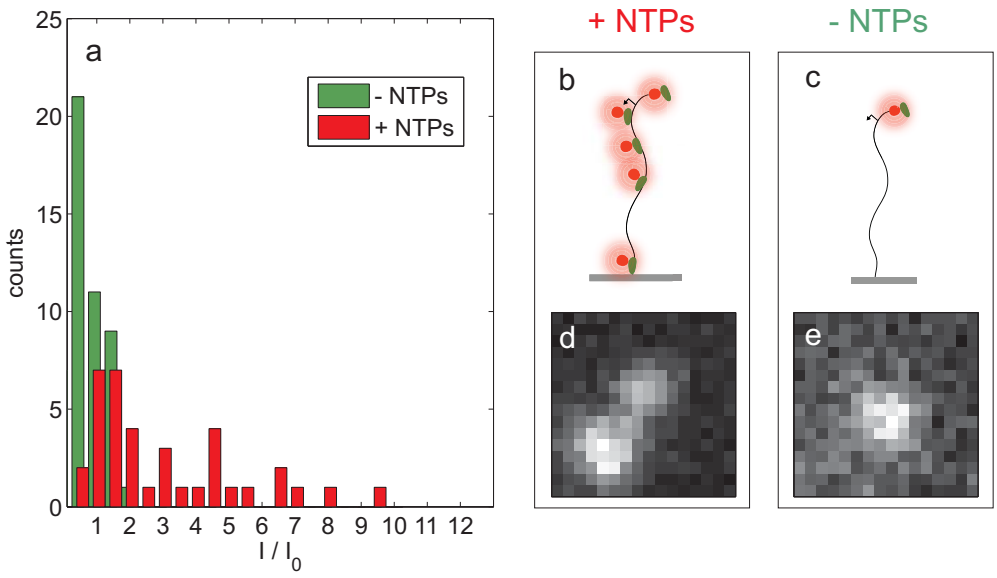

Figure 5: Activity of QD:T7RNAP complexes tested in a single molecule assay. (a) Intensity distributions of DNA tethers with varying number of QDs attached. Red bars denote an experiment with NTP present (n=39), green bars the control without NTP (n=49). The concentration of RNAPs was 200 nM. (b) Sketch of the +NTP experiment where QDs are attached both at the biotinylated end of the tether and as QD:T7RNAP complexes elongating along the tether. (c) Sketch of the -NTP control, only a single QD is attached at the biotinylated 5′ end of the tether. (d) Image of a typical +NTP experiment where QDs are actually seen at different locations along the tether. (e) Image of a typical -NTP control, only a single QD is visible.

Bibliography

[1] Jin, J. *et al.* Synergistic action of RNA polymerases in overcoming the nucleosomal barrier. *Nature Publishing Group* **17**, 745–752 (2010).

[2] Kim, J. H. & Larson, R. G. Single-molecule analysis of 1D diffusion and transcription elongation of T7 RNA polymerase along individual stretched DNA molecules. *Nucleic acids research* **35**, 3848–58 (2007).

[3] Skinner, G. M., Baumann, C. G., Quinn, D. M., Molloy, J. E. & Hoggett, J. G. Promoter binding, initiation, and elongation by bacteriophage T7 RNA polymerase. A single-molecule view of the transcription cycle. *The Journal of biological chemistry* **279**, 3239–44 (2004).

[4] Pomerantz, R. T. *et al.* A tightly regulated molecular motor based upon T7 RNA polymerase. *Nano letters* **5**, 1698–703 (2005).

[5] Larson, M. H., Greenleaf, W. J., Landick, R. & Block, S. M. Applied force reveals mechanistic and energetic details of transcription termination. *Cell* **132**, 971–82 (2008).

[6] Finkelstein, I. J., Visnapuu, M.-L. & Greene, E. C. Single-molecule imaging reveals mechanisms of protein disruption by a DNA translocase. *Nature* 1–5 (2010).

[7] F, C. Central dogma of molecular biology. *Nature* **227**, 561–563 (1970).

[8] Bai, L., Santangelo, T. J. & Wang, M. D. Single-molecule analysis of RNA polymerase transcription. *Annual review of biophysics and biomolecular structure* **35**, 343–60 (2006).

[9] Steitz, T. A. The structural changes of T7 RNA polymerase from transcription initiation to elongation. *Current opinion in structural biology* **19**, 683–90 (2009).

[10] Liu, C. & Martin, C. T. Fluorescence characterization of the transcription bubble in elongation complexes of T7 RNA polymerase. *Journal of molecular biology* **308**, 465–75 (2001).

[11] Datta, K. & von Hippel, P. H. Direct spectroscopic study of reconstituted transcription complexes reveals that intrinsic termination is driven primarily by ther-

modynamic destabilization of the nucleic acid framework. *The Journal of biological chemistry* **283**, 3537–49 (2008).

[12] Shearwin K E, Callen B P, E. J. B. Transcriptional interference -a crash course. *Trends in Genetics* **21**, 339–345 (2005).

[13] Crampton, N., Bonass, W. a., Kirkham, J., Rivetti, C. & Thomson, N. H. Collision events between RNA polymerases in convergent transcription studied by atomic force microscopy. *Nucleic acids research* **34**, 5416–25 (2006).

[14] Roucourt, B. & Lavigne, R. The role of interactions between phage and bacterial proteins within the infected cell: a diverse and puzzling interactome. *Environmental microbiology* **11**, 2789–805 (2009).

[15] A, I. Functional modulation of Escherichia Coli RNA polymerase. *Annu. Rev. Microbiol.* **54**, 499–518 (2000).

[16] Steitz, T., Smerdon, S., Jager, J. & Joyce, C. A unified polymerase mechanism for nonhomologous DNA and RNA polymerases. *Science* **266**, 2022–2025 (1994).

[17] Steitz, T. a. The structural basis of the transition from initiation to elongation phases of transcription, as well as translocation and strand separation, by T7 RNA polymerase. *Current opinion in structural biology* **14**, 4–9 (2004).

[18] Tinoco I, Sauer K, Wang J C, P. J. D. Physical Chemistry, Principles and applications in biological sciences. *Prentice Hall Inc* (2002).

[19] Dunn, M. J. Gel Electrophoresis: Proteins. *BIOS Scientific publishers Limited, UK* (1993).

[20] Sambrook J & Russel D W. Molecular cloning a laboratory manual. *Cold Spring Harbor Laboratory Press* **3rd ed.** (2001).

[21] Mittal, R. & Bruchez, M. P. Biotin-4-Fluorescein Based Fluorescence Quenching Assay for Determination of Biotin Binding Capacity of Streptavidin Conjugated Quantum Dots (2011).

[22] Electrophoresis of DNA and other polyelectrolytes: Physical mechanisms. *REVIEWS OF MODERN PHYSICS* **72**, 813–872 (2000).

[23] eha, D. *et al.* Intercalators. 1. Nature of Stacking Interactions between Intercalators (Ethidium, Daunomycin, Ellipticine, and 4,6-Diaminide-2-phenylindole) and DNA Base Pairs. Ab Initio Quantum Chemical, Density Functional Theory, and Empirical Potential Study. *Journal of the American Chemical Society* **124**, 3366–3376 (2002).

[24] McPherson, M. J. Moller, S. G. PCR. *BIOS Scientific Publishers* (2000).

[25] Boom R, Sol C J A, Salimans M M M, J. C. L. Rapid and Simple Method for Purification of Nucleic Acids. *Journal of Clinical Microbiology* **28**, 495–503 (1990).

[26] Vanzi, F., Broggio, C., Sacconi, L. & Pavone, F. S. Lac repressor hinge flexibility and DNA looping: single molecule kinetics by tethered particle motion. *Nucleic acids research* **34**, 3409–20 (2006).

[27] van den Broek, B., Vanzi, F., Normanno, D., Pavone, F. S. & Wuite, G. J. L. Real-time observation of DNA looping dynamics of Type IIE restriction enzymes NaeI and NarI. *Nucleic acids research* **34**, 167–74 (2006).

[28] Tolić-Nø rrelykke, S. F., Rasmussen, M. B., Pavone, F. S., Berg-Sø rensen, K. & Oddershede, L. B. Stepwise bending of DNA by a single TATA-box binding protein. *Biophysical journal* **90**, 3694–703 (2006).

[29] D A Schafer. Transcription by single molecules of RNA-polymerase observed by light microscopy. *NATURE* **352**, 444–448 (1991).

[30] Boal, D. Mechanics of the cell. *Cambridge university press* (2002).

[31] Ebenstein, Y. *et al.* Lighting up individual DNA binding proteins with quantum dots. *Nano letters* **9**, 1598–603 (2009).

[32] Colton, H. M. *et al.* Visualization and quantitation of peroxisomes using fluorescent nanocrystals: treatment of rats and monkeys with fibrates and detection in the liver. *Toxicological sciences : an official journal of the Society of Toxicology* **80**, 183–92 (2004).

[33] Cai, W., Chen, K., Li, Z.-B., Gambhir, S. S. & Chen, X. Dual-function probe for PET and near-infrared fluorescence imaging of tumor vasculature. *Journal of nuclear medicine : official publication, Society of Nuclear Medicine* **48**, 1862–70 (2007).

[34] Fahlman, B. D. Materials chemistry. *Springer* (2007).

[35] Peter Atkins, J. d. P. Physical chemistry. *Oxford university press, 8th ed.* (2006).

[36] He, B. *et al.* Rapid mutagenesis and purification of phage RNA polymerases. *Protein expression and purification* **9**, 142–51 (1997).

[37] Beckett, D., Kovaleva, E. & Schatz, P. J. A minimal peptide substrate in biotin holoenzyme synthetase-catalyzed biotinylation. *Protein science : a publication of the Protein Society* **8**, 921–9 (1999).

[38] Chapman-Smith, A. The enzymatic biotinylation of proteins: a post-translational modification of exceptional specificity. *Trends in Biochemical Sciences* **24**, 359–363 (1999).

[39] Durniak, K. J., Bailey, S. & Steitz, T. a. The structure of a transcribing T7 RNA polymerase in transition from initiation to elongation. *Science (New York, N.Y.)* **322**, 553–7 (2008).

[40] ExPASy ProtParam tool, Swiss Institute Of Bioinformatics URL `www.expasy.ch/tools/protparam.html`.

[41] Frazão, C. *et al.* Unravelling the dynamics of RNA degradation by ribonuclease II and its RNA-bound complex. *Nature* **443**, 110–4 (2006).

[42] Blackburn, P., Wilson, G. & Moore, S. Ribonuclease inhibitor from human placenta. Purification and properties. *J. Biol. Chem.* **252**, 5904–5910 (1977).

[43] Ouameur, A. A. & Tajmir-Riahi, H.-A. Structural analysis of DNA interactions with biogenic polyamines and cobalt(III)hexamine studied by Fourier transform infrared and capillary electrophoresis. *The Journal of biological chemistry* **279**, 42041–54 (2004).

[44] Lindemose, S. r., Nielsen, P. E. & Mø llegaard, N. E. Polyamines preferentially interact with bent adenine tracts in double-stranded DNA. *Nucleic acids research* **33**, 1790–803 (2005).

[45] Sigel, H. *et al.* Stabilities and isomeric equilibria in solutions of monomeric metal-ion complexes of guanosine 5'-triphosphate (GTP4-) and inosine 5'-triphosphate (ITP4-) in comparison with those of adenosine 5'-triphosphate (ATP4-). *Chemistry (Weinheim an der Bergstrasse, Germany)* **7**, 3729–37 (2001).

[46] Thomen, P. *et al.* T7 RNA polymerase studied by force measurements varying cofactor concentration. *Biophysical journal* **95**, 2423–33 (2008).

[47] Sperling, R., Pellegrino, T., Li, J., Chang, W. & Parak, W. Electrophoretic Separation of Nanoparticles with a Discrete Number of Functional Groups. *Advanced Functional Materials* **16**, 943–948 (2006).

[48] Clarke, S. J., Hollmann, C. A., Aldaye, F. A. & Nadeau, J. L. Effect of ligand density on the spectral, physical, and biological characteristics of CdSe/ZnS quantum dots. *Bioconjugate chemistry* **19**, 562–8 (2008).

[49] Bücking, W., Massadeh, S., Merkulov, A., Xu, S. & Nann, T. Electrophoretic properties of BSA-coated quantum dots. *Analytical and bioanalytical chemistry* **396**, 1087–94 (2010).

[50] Pernodet, N., Maaloum, M. & Tinland, B. Pore size of agarose gels by atomic force microscopy. *Electrophoresis* **18**, 55–8 (1997).

[51] Westermeier, R. Electrophoresis in practice. *Wiley-vch 3rd ed.* (2001).

[52] online pI calculators:. *http://vitalonic.narod.ru/biochem/index_en.html; http://www.scripps.edu/~cdputnam/protcalc.html; http://www3.embl.de/cgi/pi-wrapper.pl* .

[53] Zhang, H. *et al.* Fluorescent tumour imaging of type I IGF receptor in vivo: comparison of antibody-conjugated quantum dots and small-molecule fluorophore. *British journal of cancer* **101**, 71–9 (2009).

[54] Han, L. *et al.* Calibration of Tethered Particle Motion Experiments. *Springer, New York* **150**, 123–138 (2009).

[55] Jauffred, L., Sletmoen, M., Czerwinski, F. & Oddershede, L. Quantum dots as handles for optical manipulation. *SPIE proceeding* **7762**, 2–9 (2010).

[56] Milne, G. StAT, St Andrews Tracker (2009). URL `//faculty.washington.edu/gmilne/tracker.htm`.

[57] Nelson, P. C. *et al.* Tethered particle motion as a diagnostic of DNA tether length. *The journal of physical chemistry. B* **110**, 17260–7 (2006).

[58] Jauffred, L. Optical manipulation and biological applications of quantum dots. *PhD Thesis* (2010).

[59] Segall, D., Nelson, P. & Phillips, R. Volume-Exclusion Effects in Tethered-Particle Experiments: Bead Size Matters. *Physical Review Letters* **96**, 1–4 (2006).

[60] Milstein, J. N., Chen, Y. F. & Meiners, J.-C. Bead size effects on protein-mediated DNA looping in tethered-particle motion experiments. *Biopolymers* **95**, 144–50 (2011).